Fluorescence-activated cell sorting as a method to isolate ionocyte populations from gill tissue

Ibragim El-Sakhli

Thesis submitted to the

Faculty of Science

University of Ottawa

In partial fulfillment of the requirements for the

Master of Science degree in the

Ottawa-Carleton Institute of Biology

Abstract

In freshwater fish, such as the rainbow trout (*Oncorhynchus mykiss*), higher ion concentrations in the body fluids relative to the dilute surrounding environment lead to diffusive ion loss that is countered by active ion uptake. Active ion uptake is achieved via specialised cells in the gill epithelium known as ionocytes, with the species studied to date exhibiting multiple ionocyte subtypes with specific complements of ion transport proteins. To better understand the functions and responses of each ionocyte subtype, methods are needed to isolate specific ionocyte subtypes. This thesis developed a method to use fluorescence-activated cell sorting (FACS) to isolate the peanut lectin agglutinin-positive (PNA^+) ionocyte subtype of the trout gill, which is posited to be a base-secreting cell that takes up Cl^- ions. A suspension of gill cells dissociated using ethylenediaminetetraacetic acid (EDTA) was labelled with biotinylated PNA that was detected using streptavidin conjugated to a fluorophore, and subjected to FACS to yield a population of PNA^+ ionocytes of high viability and purity. To validate the utility of the approach, it was used in a proof-of-principle experiment to evaluate transcript abundance of cytosolic carbonic anhydrase (CAc) in PNA^+ ionocytes in trout that were subjected to metabolic alkalosis. This experiment revealed that the relative transcript abundance of CAc was significantly elevated in PNA^+ ionocytes of alkalotic trout relative to that of control trout (P = 0.001; N = 7), a response that is consistent with the expected role of PNA^+ ionocytes in compensation for systemic alkalosis.

Résumé

Pour les poissons d'eau douce, comme la truite arc-en-ciel (*Oncorhynchus mykiss*), les concentrations plus élevées des ions par rapport à celles dans l'environnement avoisinant entraîne une perte des ions par diffusion qui peut être compensée par l'absorption active des ions. L'absorption active des ions est réalisée grâce à des cellules spécialisées dans l'épithélium des branchies, appelées des ionocytes, dont plusieurs sous-types existent. Afin de mieux comprendre les fonctions et les réponses de chaque sous-type d'ionocyte, une méthodologie est nécessaire pour isoler des sous-types spécifiques. Cette thèse décrit une méthode basée sur le triage des cellules à fluorescence (« FACS » pour « Fluorescence-activated cell sorting ») pour l'isolation d'un sous-type d'ionocyte des branchies des truites qui exprime PNA (pour « peanu lectin agglutinin »; une agglutinine) et avancé comme les cellules qui reprend les ions Cl^-. Une suspension mixte des cellules de branchies, dissociées avec l'éthylènediaminetétraacétique (EDTA), a été étiquetée avec PNA biotinylée, puis étiquetée avec la streptavidine conjuguée à un fluorochrome. Ensuite, ces cellules ont été triées par FACS et, enfin, une population pure et viable des ionocytes PNA^+ a été isolée. Afin de valider l'utilité de cette technique, une expérience de preuve du principe a été conçue et exécutée utilisant des truites exposées à l'alcalose métabolique et mesurant les niveaux de l'anhydrase carbonique cytosolique (« *cac* » pour « cytosolic carbonic anhydrase ») dans leurs populations d'ionocytes PNA^+. Cette expérience révèle que l'abondance relative du transcrit *cac* a été élevée dans une manière significative chez les ionocytes PNA^+ des truites mis en état d'alcalose par rapport aux niveaux mesurés dans les contrôles ($P = 0.001$, $N = 7$). Cette réponse conforme au rôle attendu des ionocytes PNA^+ dans la compensation pour l'alcalose systémique.

Table of Contents

Acknowledgements

First and foremost, I would like to thank my supervisors, Drs Katie Gilmour and Steve Perry, for giving me this opportunity to work and learn under their guidance . Thank you for your brilliant advice and unwavering support even at my low points, without which this project would have never succeeded. Also a huge thanks to my committee members, Drs Michael Jonz and Jan Mennigen. Thank you for looking over my work and giving your suggestions.

Next, I would like to thank all the lab members of Perry and Gilmour labs, for their support and help with my project. Special thanks to KS, HMY and AZ for always being there for me and helping with whatever questions came up.

Big thanks to Peter Andrew Ochalski, Phillip Pelletier, Shahrokh Ghobadloo, Vera Tang, Bill Fletcher, Gabriel Guillet and Alp Oran for helping me with various techniques involved in my experiments as well as teaching me new things on daily basis.

I would also like to thank my family for always being there for me, supporting me emotionally and with great advices. Without them I wouldn't be where I am today.

Last, but not least I would like to thank Kesiah Stoker for being my support wall every day throughout this journey. Thank you for always being there for me no matter what. And also a special thanks to Jay for providing constant entertainment and distractions!

List of Figures and Tables

List of Abbreviations

Abbreviation	Full Name
ANOVA	Analysis of variance
ATP	Adenosine triphosphate
CAc	Cytosolic carbonic anhydrase
ClC	Cl^- channel
CCAC	Canadian Council on Animal Care
cDNA	Complementary deoxyribonucleic acid
DAPI	4′,6′-diamidino- 2-phenylindole
ECaC	Epithelial Ca^{2+} channel
EDTA	Ethylenediaminetetraacetic acid
EF1α	Elongation factor 1 alpha
ENaC	Epithelial Na^+ channel
FACS	Fluorescence-activated cell sorting
FITC	Fluorescein isothiocyanate
FW	Freshwater
HR	H^+-ATPase rich cell
IC	Intercalated cell
KS	K^+-secreting cell
MACS	Magnetic cell separation
NaR	Na^+/K^+-ATPase rich cell
NCC	Na^+/Cl^- co-transporter rich cell
NCX	Na^+/Ca^{2+} exchanger

NHE	Na^+/H^+ exchanger
NKA	Na^+/K^+-ATPase
PBS	Phosphate buffered saline
PCR	Polymerase chain reaction
PFA	Paraformaldehyde
pHi	Intracellular pH
PMCA	Ca^{2+}-ATPase
PNA	Peanut lectin agglutinin
RBC	Red blood cell
RT-PCR	Reverse transcriptase polymerase chain reaction
SLC	Solute carrier

Chapter 1 INTRODUCTION

1.1 Overview

Although in recent years our understanding of the ion-transporting cells or ionocytes of the fish gill has greatly expanded (e.g. Dymowska et al., 2012, Hiroi and McCormick, 2012; Guh et al., 2015), progress addressing the many questions that remain has been hindered by the lack of methods to isolate specific ionocyte types for study, with much research relying instead on quantifying responses in tissue homogenates. Thus, the goal of the present study was to isolate a specific ionocyte type, the peanut lectin agglutinin-positive (PNA^+) ionocyte of the rainbow trout (*Oncorhynchus mykiss*) gill, as a distinct cell population and, as proof-of-principle, to investigate the response of cytosolic carbonic anhydrase (CAc) to the acid-base challenge of systemic alkalosis within this ionocyte type. The use of fluorescence-activated cell sorting (FACS) as a means of achieving a relatively pure population of PNA^+ cells was developed to overcome the issues associated with assessing transcript abundance in gill homogenates, the method typically used in previous studies of acid-base responses in rainbow trout. Following on from a recent study that used immunohistochemistry to demonstrate increased abundance of CAc-positive PNA^+ ionocytes in the gill of trout exposed to metabolic alkalosis (Brannen and Gilmour, 2018), the goal of the present study was to test the hypothesis that transcriptional regulation of *cac* contributes to this response. Based on this hypothesis, transcript abundance of *cac* would be predicted to be significantly higher in the PNA^+ ionocytes of rainbow trout that had been exposed to alkalosis compared to those of fish held under control conditions. The significance of this study lies in its focus on acid-base responses at the cellular level. By making use of FACS to generate PNA^+ cell fractions of high purity, insight can be gained into the mechanism of regulation of CAc in a specific ionocyte type. Thus, this study also serves as a proof-of-principle

in terms of using FACS to allow acid-base responses to be studied at the cellular rather than tissue level.

1.2 Osmoregulation and acid-base balance in freshwater fishes

Living in a wide range of aquatic environments, fishes experience diversity in terms of water pH ranges and ion concentrations (Evans et al., 2005). For example, freshwater fish such as the rainbow trout maintain body NaCl concentrations of ~150 mmol L^{-1} whereas the NaCl concentration of fresh water typically is less than 1 mmol L^{-1}. This concentration difference results in a diffusion gradient such that freshwater fishes lose ions to the environment by diffusion, primarily across the gill which must be relatively permeable to allow adequate respiratory gas transfer to occur (Smith, 1932; Krogh, 1939; Girard and Payan, 1980). Diffusive ion loss is accompanied by osmotic water gain, and freshwater fish therefore use several physiological mechanisms to eliminate excess water and replace lost ions. Osmotic water gain is countered by the production of large volumes of dilute urine (Smith, 1932). To counter ion losses, freshwater fishes actively take up ions from their dilute environment using specialised ion-transporting cells that, in adult fish, are located primarily in the gill epithelium (Zadunaisky, 1996; Evans et al., 2005; Hwang et al., 2011; Kumai and Perry, 2012). Known in the older literature as freshwater chloride cells or mitochondrion-rich cells (Zadunaisky, 1996; Perry, 1997), the ion-transporting cells now are termed ionocytes and express a complement of ion channels, transporters and enzymes to achieve the transepithelial transport of one or more specific ions across the gill epithelium. In addition to their role in ion regulation, ionocytes are also believed to be a major player in acid-base regulation (Cameron and Iwama, 1987; Goss et al., 1998; Claiborne et al., 2002). Teleost fish typically regulate extracellular pH by adjusting plasma HCO_3^- levels through the differential regulation of H^+ and HCO_3^- effluxes across the gill,

with the kidney playing a supporting role in the retention of filtered HCO_3^- (Claiborne et al., 2002; Marshall, 2002; Hirose et al., 2003; Perry et al., 2003b; Evans et al., 2005). For example, compensation for a systemic acidosis involves accumulating HCO_3^- by increasing branchial net acid excretion, through increased H^+ excretion (which is linked to Na^+ uptake) and/or decreased HCO_3^- excretion (which is linked to Cl^- uptake). During a systemic alkalosis, by contrast, HCO_3^- excretion via both gill and kidney is increased (Goss and Wood, 1991; Goss and Perry, 1994; Wood et al., 1999). By analogy with other epithelia involved in the regulation of both ionic and acid-base balance, such as the mammalian nephron (Star et al., 1985; Emmons and Curtz, 1994), it would be expected that distinct ionocyte types are responsible for Na^+ uptake linked to acid excretion, and Cl^- uptake linked to base excretion. Indeed, multiple subtypes of ionocytes have now been recognized in several fish species, with the classification of ionocytes being based upon the suite of transporters/ion channels expressed.

The freshwater fish species that have been studied to date possess at least two types of ionocytes, including an acid-secreting ionocyte that takes up Na^+ ions, and a base-secreting ionocyte that is hypothesized to take up Cl^- ions (Avella and Bornancin, 1989; Lin and Randall, 1991; Wright and Wood, 2009; Dymowska et al., 2012). However, different species of freshwater fish appear to possess different numbers and types of ionocytes (Hwang et al., 2011; Dymowska et al., 2012), making the establishment of specific mechanisms responsible for ion uptake and pH regulation more complicated. For example, five types of ionocytes have been characterized in zebrafish (*Danio rerio*) to date; the proton pump-rich or HR cell that takes up Na^+ in exchange for acid excretion, the Na^+, K^+-ATPase (NKA)-rich or NaR cell that is responsible for Ca^{2+} uptake, the Na^+, Cl^- cotransporter-expressing or NCC cell that contributes to the uptake of both Na^+ and Cl^- without the involvement of acid-base equivalents, the solute

carrier 26 (SLC26) cell that takes up Cl^- in exchange for base excretion, and the K^+ secreting or KS cell that excretes K^+ (Hwang et al., 2011). In tilapia (*Oreochromis mossambicus*) acclimated to freshwater conditions, three types of ionocytes have been identified to date; type I ionocytes that express basolateral NKA, type II ionocytes that couple basolateral NKA with apical expression of NCC, and type III ionocytes in which basolateral NKA and Na^+-K^+-$2Cl^-$ cotransporter (NKCC) are co-expressed with apical Na^+-H^+ exchanger 3 (NHE3) (Hiroi et al., 2008; Inokuchi et al., 2009). In zebrafish, the proposed acid-secreting cell is the HR cell (Hwang et al., 2011), whereas in tilapia, it is the type III ionocyte (Hiroi et al., 2005), and in both cell types, acid secretion has been proposed to be coupled to Na^+ uptake. Similarly, in medaka the NHE ionocyte has been proposed to carry out acid secretion through the NHE3 exchanger (Hsu et al., 2014). All three species also possess an ionocyte that expresses apical NCC (Hiroi et al., 2005; Hwang et al., 2011; Hsu et al., 2014), which is also present in an ionocyte of killifish (Katoh et al., 2001; Kaneko, 2003). To date, however, an SLC26-expressing cell that links base secretion and Cl^- uptakehas been detected only in zebrafish (Hwang et al., 2011). Although there are similarities among these species with respect to the types of ionocytes that are present, differences are also apparent, from the number of ionocyte types that have been identified to date (five in zebrafish versus three in tilapia and medaka) to the possible absence or presence of unique transporters. For example, killifish ionocytes do not seem to possess a chloride transporter other than NCC (Katoh et al., 2001; Kaneko, 2003). These findings point to a certain degree of variability in ionocytes among species, but also to similarities in the ion-transporting mechanisms of these ionocytes.

1.3 Ionocytes of the rainbow trout gill epithelium

Current thought suggests that the rainbow trout has only two distinct types of ionocytes, PNA^+ and PNA-negative (PNA^-) cells (Goss et al., 2001), that are distinguished on the basis of whether they bind PNA (Fig. 1.1). Peanut agglutinin is a plant lectin protein, which specifically binds to certain carbohydrate sequences (Novogrodsky et al., 1975). Plant lectins generally function *in vivo* for defence against foreign objects and toxins, communication between plant cells and beneficial microorganisms (symbiosis), and elongation of cell walls (Etzler, 1986), but they also are used as a scientific tool, specifically as a biological marker for cell types that they recognize. In mammals, PNA was used to differentiate between alpha- and beta-intercalated cells of the mammalian nephron that are effectively the acid and base secreting cells of the kidney, respectively, because it was found to bind selectively to beta-intercalated kidney cells (ICs) but not to alpha ICs (LeHir et al., 1982). The main function of beta ICs is to secrete HCO_3^- into the urine under conditions of alkalosis (Emmons and Curtz, 1994), with bicarbonate ion transport being achieved through pendrin, a Cl^-/HCO_3^- exchanger (Emmons and Curtz, 1994). By contrast, alpha ICs secrete protons into the urine under conditions of acidosis through H^+-ATPases (Star et al., 1985). Note that in mammals, the kidney plays a key role in the regulation of acid-base balance (unlike in fish where the role of the kidney is to support the regulation of acid-base balance that occurs at the gill; see above), and therefore HCO_3^- (to correct an alkalosis) or H^+ (to correct an acidosis) secretion into urine is a key process for acid-base compensation (Schwartz et al., 1985; Gao et al., 2010).

Goss and colleagues (2001) discovered that PNA selectively binds to one population of ionocytes in the rainbow trout gill, but not to a second, thereby providing evidence for two distinct ionocyte types in the trout gill epithelium. Goss et al. (2001) hypothesized that PNA^+

cells, by analogy to beta ICs, would function as base-secreting cells, secreting HCO_3^- through Cl^-/HCO_3^- exchangers and playing a role in lowering pH in fish experiencing a systemic alkalosis. Morphological characterization of the PNA^+ cells revealed features typical of those of what were known at the time as freshwater chloride cells, i.e. these cells were found at the base of the lamellae and were mitochondrion- and membrane-rich (Goss et al., 2001). As yet, there is relatively little experimental support for a base-secreting role for PNA^+ cells, although a recent report of changes in PNA^+ cells in response to systemic alkalosis is suggestive (Brannen and Gilmour, 2018). The presence of a Cl^-/HCO_3^- mechanism in these cells has yet to be demonstrated. On the other hand, PNA^- cells were proposed to act like alpha ICs, secreting H^+ in fish experiencing a systemic acidosis through H^+-ATPases linked to Na^+ uptake (Goss et al., 2001). Supporting this role for PNA^- cells, western blot analysis revealed that PNA^- ionocytes expressed H^+-ATPase that increased in abundance in fish exposed to an acidosis (Galvez et al., 2002). Moreover, experiments using the inhibitors bafilomycin and phenamil, which act on H^+ ATPase and Na^+ channels, respectively, revealed that PNA^- ionocytes possessed bafilomycin- and phenamil-sensitive Na^+ uptake (Goss et al., 2001; Galvez et al., 2002; Reid et al., 2003).

To provide insight into the proposed roles of ionocyte subtypes in ion and acid-base balance, several studies have investigated PNA^+ and PNA^- ionocytes with a view to characterizing the complement of ion-transporting proteins that each cell type expresses. Galvez et al. (2002) utilized the magnetic cell separation technique (MACS) together with Percoll density separation to isolate PNA^+ and PNA^- ionocytes and showed through Western blotting experiments on the separated cells that both cell types exhibit NKA, while the PNA^- ionocyte exhibits twice the protein abundance of H^+-ATPase as the PNA^+ ionocyte.

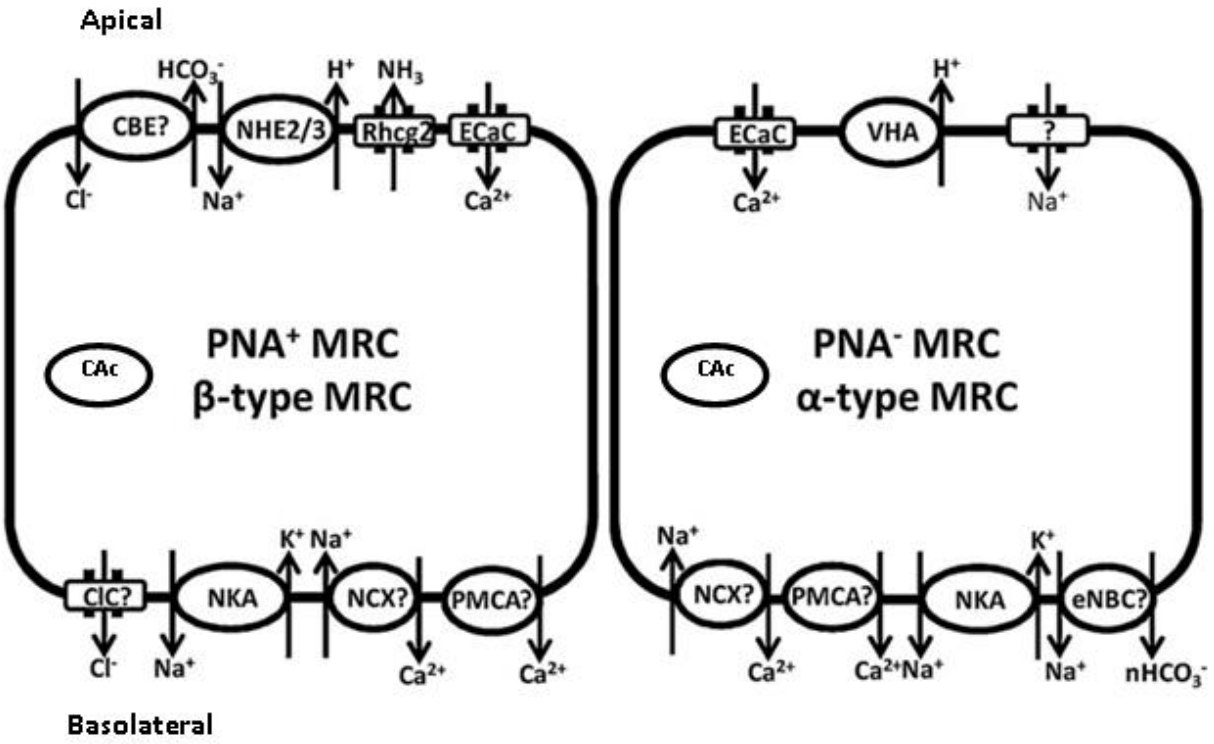

Figure 1.1. A schematic depicting the two types of ionocytes thought to be present in rainbow trout (*Oncorhynchus mykiss*) gill, and the complement of ion channels and transporters that has been proposed for each type. Peanut lectin agglutinin-positive (PNA^+) cells have been proposed to express a Cl^-/HCO_3^- exchanger (CBE), Na^+-H^+ exchangers 2 and 3 (NHE2/3), Rh glycoprotein 2 (Rhcg 2) and the epithelial Ca^{2+} channel (ECaC) on the apical membrane, cytosolic carbonic anhydrase (CAc) in the cytosol, and Na^+-H^+-ATPase (NKA), Na^+/Ca^{2+} exchanger (NCX), Ca^{2+}-ATPase (PMCA) and Cl^- channels (ClC) on the basolateral membrane. Peanut lectin agglutinin negative ionocytes (PNA^-) are proposed to express ECaC and V-type H^+-ATPase (VHA) on the apical membrane as well as an unknown Na^+ channel, CAc in the cytosol, and NKA, Na^+/Cl^- co-transporter (eNBC), PMCA and NCX on the basolateral membrane. Those identified with a question mark represent proposed transporters or channels for which empirical support is limited or currently lacking. (Modified from Dymowska et al., 2012.)

Galvez and colleagues (2002) also reported that H^+ ATPase expression in PNA^- ionocytes significantly increased in response to hypercapnia, as well as no change in expression in response to metabolic alkalosis.

A subsequent study by Reid and colleagues (2003) used the method of separation designed by Galvez et al. (2002) to study Na^+ uptake in PNA^+ versus PNA^- ionocytes. Using isolated ionocyte populations, Reid and colleagues (2003) inhibited H^+-ATPase with bafilomycin and an effect on Na^+ uptake only in PNA^- ionocytes, providing further support for the presence of H^+-ATPase in PNA^- ionocytes. Acidification stimulated Na^+ uptake in PNA^- but not PNA^+ ionocytes, and this acidification-induced Na^+ uptake was inhibited by phenamil, an inhibitor of epithelial Na^+ channels (Reid et al., 2003). These data suggest the presence in PNA^- ionocytes of a H^+-ATPase-Na^+ channel mechanism for Na^+ uptake (Reid et al., 2003).

Parks and colleagues (2009) investigated cellular Cl^- transport in both ionocyte types using measurements of intracellular pH (pHi) for isolated ionocytes in a Cl^--free environment. They observed that pHi increased in both PNA^+ and PNA^- cells exposed to Cl^--free conditions, suggesting the presence of a Cl^-/HCO_3^-exchanger in both cell types, because in the absence of chloride in the external environment, anion exchangers would be expected to transport intracellular chloride out of the cell in exchange for bicarbonate, thus raising pHi. Parks et al. (2009) suggested PNA^+ cells would express the anion exchanger apically, for transepithelial Cl^- uptake and HCO_3^- secretion, whereas PNA^- cells would express the anion exchanger basolaterally for the purpose of pHi regulation.

An alternative to the H^+ pump-Na^+ channel mechanism for Na^+ uptake at the fish gill is a mechanism based on Na^+/H^+ exchangers (NHE). With freshwater Na^+ concentrations being much

lower than those of the body fluids of freshwater fish, how this exchanger can function for Na^+ uptake is not obvious (Girard and Payan, 1980; Parks et al., 2008). To overcome the apparent thermodynamic constraints, a model was proposed by Wright and Wood (2009) in which NHE2/3 forms a metabolon with the ammonia transport protein Rh glycoprotein 2 (Rhcg 2). Like other members of the Rh glycoproteins, Rhcg 2 is believed to function as an ammonia channel (Nakada et al., 2007; Nawata et al., 2007). In this "ammonia trapping" model, Rhcg 2 and NHE2/3 as well as a proton pump work together as a "metabolon", where Rhcg 2 strips a proton from NH_4^+ to create NH_3 which can then exit the cell down its partial pressure gradient via Rhcg 2, while the proton is used either by NHE2/3 to bring in Na^+, or by a H^+ pump to create a gradient for Na^+ entry via a channel (e.g. ASIC) (Wright and Wood, 2012). Tsui et al. (2008) provided experimental support for this model with trout gill cell cultures by reporting that apical treatment of a polarized cell layer with low Na^+ conditions led to an increase in the relative mRNA expression of Rhcg 2. Kumai and Perry (2011) provided further support for this mechanism by showing that knockdown of Rhcg 1 (a different isoform of Rhcg found in zebrafish) in zebrafish larvae led to significant reductions not only in ammonia excretion, but also in Na^+ uptake. Given their involvement in Na^+ uptake in exchange for H^+ secretion, NHE exchangers would be expected to be present in acid-secreting cells. For example, NHE has been localized to HR cells in zebrafish (Hwang, 2009) and type III ionocytes in tilapia (Hiroi et al., 2008), both cells types that play a role in Na^+ uptake and proton secretion. Interestingly, however, NHE2 and NHE3 were localized to PNA^+ but not PNA^- ionocytes in rainbow trout (Ivanis et al., 2008; Hiroi and McCormick, 2012).

1.4 Research objectives

If PNA^+ and PNA^- ionocytes in the gill epithelium of rainbow trout do indeed serve to secrete base and acid, respectively, then both cell types would be predicted to express cytosolic carbonic anhydrase (CAc) (Gilmour and Perry, 2009). Carbonic anhydrase is a zinc metalloenzyme that catalyzes the reversible chemical reactions of CO_2 and water, $CO_2+H_2O\leftrightarrow H^+ +HCO_3^-$, and therefore plays key roles in ionic regulation and acid-base balance among other physiological processes (Maren, 1967; Gilmour and Perry, 2009; Boone et al., 2014). In rainbow trout, two isoforms of CA have been reported to be expressed in the cytoplasm of cells, CAb, which appears to be expressed specifically in red blood cells, and CAc, which is broadly expressed in a range of tissues, including the gill, where it is expressed in high abundance (Esbaugh et al., 2005). Current models for ion uptake linked to the excretion of acid-base equivalents suggest that CAc should be present in both PNA^+ and PNA^- cells of the trout gill epithelium, to catalyze the hydration of CO_2 as it diffuses across the gill epithelium, providing the protons and bicarbonate ions needed by the two cell types for ion uptake (Gilmour and Perry, 2009). Goss et al. (2011) reported that CA activity in PNA^- ionocytes was inhibited by silver, a finding that supports the presence of CA in PNA^- ionocytes. Boyle et al. (2015) reported a decrease in Cl^- uptake in trout embryos treated with the CA inhibitor acetazolamide, which provides indirect support for the presence of CA in PNA^+ ionocytes. However, a recent study reported on the basis of an immunohistochemical analysis of trout gill tissue that less than 5% of PNA^+ cells expressed CAc under control conditions, although more than 90% of PNA^-cells were immunopositive for CAc (Brannen and Gilmour, 2018). The observation of Brannen and Gilmour (2018) that most PNA^+ ionocytes lacked CAc immunostaining under control conditions was unexpected and raises questions about the role of this cell type in ionic and acid-base

regulation. Brannen and Gilmour (2018) also observed that the abundance of PNA^+ ionocytes that were immunopositive for CAc increased significantly in trout experiencing an alkalosis, supporting a role for PNA^+ cells in base secretion. Thus, the objective of the current study was to investigate the expression of CAc in PNA^+ ionocytes, and to determine whether metabolic alkalosis increases the expression of *cac* in PNA^+ ionocytes through transcriptional regulation that is specific to this ionocyte type.

Despite the information that has been gained regarding the function of rainbow trout ionocytes, there are still gaps in our knowledge of ion uptake and acid-base regulation by these cells. These knowledge gaps reflect, at least in part, methodological limitations of the research carried out to date. A key limitation is that previous research has relied largely on gill homogenates to investigate responses to acid-base disturbances, an approach that does not allow cell types responding to an acid base challenge to be differentiated. For example, Georgalis et al. (2006) reported that *cac* relative mRNA levels in gill tissue increased following exposure of rainbow trout to hypercapnia. Although this study clearly demonstrated the importance of gill CAc in responses to acid-base challenges, deductions cannot be made regarding the cell types responsible for this effect. In another example, Gilmour et al. (2011) found that gill *cac* transcript abundance decreased in trout subjected to acid infusion and increased in trout infused with base, yet the proposed model for CAc suggests that it plays an important role in compensatory responses under both conditions. Thus, the results of Gilmour et al. (2011) likely reflect opposing responses of *cac* transcript abundance in different ionocyte types within the gill epithelium, which cannot be distinguished when gill tissue is probed. Clearly, separation of cell types is necessary to fully understand the responses of the gill to acid-base disturbances. The recent work of Brannen and Gilmour (2018) tried to overcome the problem using

immunohistochemistry to evaluate cell types expressing CAc protein under different conditions. However, this method does not provide the detailed quantitative information on CAc transcript abundance or protein levels that is needed to establish mechanisms of function. Galvez et al. (2002) developed a magnetic bead separation technique to isolate both PNA^- and PNA^+ ionocytes. Suspensions of dissociated gill cells were first separated into fractions of different density based on a Percoll gradient, and the fraction containing mitochondrion-rich cells was then separated into PNA^- and PNA^+ fractions using PNA conjugated to iron particles to label cells, which were then applied to the magnetic column. With this approach, Galvez et al. (2002) reported high purity of isolated ionocytes (>95%). This approach was used in subsequent studies by the same group of workers (Reid et al., 2003) and a few others (Shahsavarani et al., 2006), but has not been widely adopted because it is difficult to use successfully.

Given the above background, the objective of the present thesis was to test the hypothesis that transcriptional regulation of *cac* occurs in the ionocytes of the gill epithelium when a rainbow trout experiences acid-base challenges. Based on this hypothesis, *cac* transcript abundance would be predicted to be significantly higher in the PNA^+ ionocytes of rainbow trout exposed to metabolic alkalosis compared to that in PNA^+ ionocytes of trout held under control conditions. The present research tested this prediction by isolating PNA^+ ionocytes from alkalotic and control rainbow trout and measuring *cac* transcript abundance. To isolate PNA^+ ionocytes, FACS and flow cytometry techniques were adopted.

1.5 Experimental approaches

In flow cytometry, light passage through cells that have been differentially labelled with fluorescent dyes allows distinct cell populations present within a sample to be quantified (Bonner et al., 1975). A sample is analyzed cell-by-cell to generate a plot of forward scatter by side scatter for all cells in the sample, where forward scatter reflects the relative size of the cell, while side scatter reflects granularity, or the organelle content of the scanned cell (Bonner et al., 1975; Laerum and Farsund, 1981; Darzynkiewicz et al., 2004). Constant detection of the laser beam is interrupted by cells going through it, and cell size is then estimated through the scatter of the laser rays by the cells as captured by forward detectors. Similarly, as cells go through the laser, light is reflected by organelles and captured by side detectors, with the degree of scatter being dependent upon the organelle content of the cell (Bonner et al., 1975; Laerum and Farsund, 1981; Darzynkiewicz et al., 2004). Fluorescence is detected by having a laser of wavelength absorbed by the fluorochrome in the sample. The excited fluorochrome emits fluorescence which is then captured by a detector within the FACS apparatus. Collectively, this approach allows all cells in the sample to be categorized by size, granularity and fluorescence (if any labels are applied), permitting specific cell populations to be identified and the number of cells in such populations to be quantified. Flow cytometry has been used effectively on trout gill tissue in previous studies. For example, Castro et al. (2014) used flow cytometry to identify CCR7 chemokine receptor-positive cells in rainbow trout gill, and Shao et al. (2010) successfully followed the disappearance of a cell population with flow cytometry following gill injury induced by exposure of the fish to brominated diphenyl ether 47.

Fluorescence-activated cell sorting takes this technique a step further to isolate cells belonging to a given population. It uses lasers to identify specific cells by the fluorescence

associated with a cell marker that is added to the sample, and a charge is applied to these cells. The cells then pass between magnets and are separated based on the applied charge (Bonner et al., 1975; Parks and Herzenberg, 1984; Wolff et al., 2003) (Fig. 1.2). Because cells are separated into different populations depending on their fluorescent labels, the purity of the isolated cell population depends on the specificity of the cell labelling (Bonner et al., 1975; Parks and Herzenberg, 1984; Wolff et al., 2003). Although FACS has not been used on rainbow trout gill cell populations to date, it has been used successfully in other cases, such as to isolate IgM-positive cells in turbot lymphoid tissue (Feng et al., 2009). The use of FACS on trout gill cell populations will allow the study of specific cell types, with PNA^+ cells being the main target of this project. Because PNA binds specifically to PNA^+ cells (Goss et al., 2001), it is expected to be a suitable marker on which to sort gill cell suspensions so as to obtain a high purity sample of PNA^+ cells.

To expose rainbow trout to metabolic alkalosis, recovery from hypercapnia will be used (Wood and Jackson, 1980; Goss and Wood, 1990; Goss et al., 1994; Brannen and Gilmour, 2018). Trout exposed to elevated partial pressures of CO_2 for a 3-day period will experience respiratory acidosis owing to increased blood PCO_2. This respiratory acidosis leads, in turn, to compensatory accumulation of HCO_3^- via the gills and kidney, such that by the end of the 3-day exposure period, trout exhibit elevated PCO_2 but normal pH – in other words, the fish is in a state of compensated acidosis (Perry et al., 1987; Goss and Perry, 1993).When the fish is returned to normocapnic conditions, it rapidly loses CO_2 by diffusion across the gill, but because HCO_3^- loss is slower than CO_2 loss, the fish experiences a temporary excess of HCO_3^- ions, resulting in a transient metabolic alkalosis until the HCO_3^- load is cleared from the body fluids via compensatory mechanisms at the gill and kidney (Perry et al., 1987; Goss and Perry, 1993).

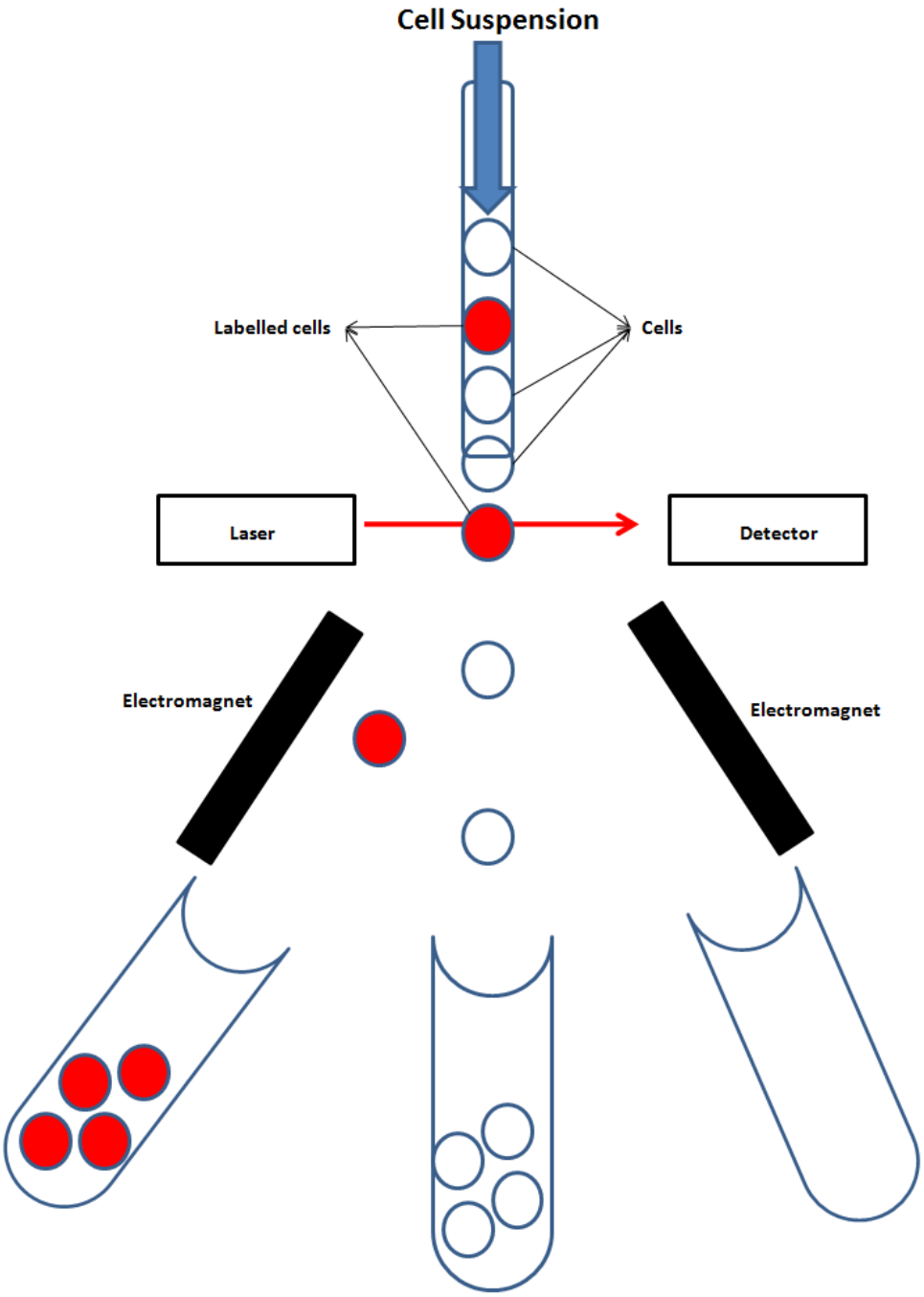

Figure 1.2. Schematic showing how a fluorescence-activated cell sorter generates isolated populations of distinct cell types.

Brannen and Gilmour (2018) utilised this technique to examine the impact of metabolic alkalosis on CAc immunohistochemistry in the trout gill. In the present study, cells were harvested for FACS and subsequent real-time RT-PCR following exposure of trout to this hypercapnic recovery paradigm, or to control conditions. In addition to assessing *cac* transcript abundance, the transcript abundances of *nka* and *nhe2/3* were examined. These transporters were selected for study because they are expressed by PNA^+ cells (Ivanis et al., 2008; Dymowska et al., 2012), but are not expected to show changes during a metabolic alkalosis because they are not known to play roles in base excretion or Cl^- uptake.

In summary, this thesis aimed to develop an effective and straightforward technique for isolating populations of rainbow trout ionocytes, to allow for future studies to be carried out on specific cell types instead of whole tissue. As a proof-of-principle, the methods developed were applied to the question of whether transcriptional regulation of *cac* occurs in trout gill ionocytes in response to an acid-base challenge. Thus, this thesis also attempted to provide insight into the mechanisms of acid-base regulation in rainbow trout.

Chapter 2 MATERIALS AND METHODS

2.1 Experimental animals

Rainbow trout, *Oncorhynchus mykiss* (mass 230 ± 9 g, mean±s.e.m., N = 42), purchased from Linwood Acres Trout Farm (Campbellcroft, ON, Canada), were transported to the University of Ottawa where they were held in 1275 L fibreglass tanks. The holding tanks were supplied with flowing, aerated, dechloraminated city of Ottawa tap water (0.25 $mmolL^{-1}$ Ca^{2+}, 0.78 $mmolL^{-1}$ Na^{+}, 0.02 $mmolL^{-1}$ K^{+}, 0.19 $mmolL^{-1}$ Cl^{-}, pH 7.6) at 13°C. The photoperiod was kept at 12 h light:12 h dark and fish were fed commercial trout pellets at a ration of 0.5% body mass per day. Trout were acclimated to these holding conditions for at least 2 weeks prior to experimentation. All experimental protocols were approved by the institutional animal care committee (protocol BL-2118) and were in compliance with the guidelines of the Canadian Council on Animal Care (CCAC) for the use of animals in research and teaching.

2.2 Development of a protocol for trout gill cell dissociation

As a starting point, the procedure adopted to generate suspensions of dissociated gills cells was that used by Shahsavarani et al. (2006), which in turn was based on the work of Goss and colleagues (Goss et al., 2001; Galvez et al., 2002). Several aspects of this protocol were modified to improve cell viability and yield. For clarity, the final protocol will be detailed first, followed by brief descriptions of the approaches that were attempted in developing this final protocol. A fish was removed from the holding tank and euthanized by a cephalic blow. The gill basket was removed from the fish and placed in ice-cold phosphate-buffered saline (PBS), and the filaments were then removed from all arches. The filaments were cut into small pieces and placed into a 50 mL Falcon tube containing 20 mL of L-15 media (ThermoFisher Scientific,

Ottawa, ON, Canada) and 200 µL of 0.5 M ethylenediaminetetraacetic acid (EDTA; ThermoFisher Scientific, Ottawa, ON, Canada). The tube was incubated on a rocking shaker (Reliable Scientific, Cambridge, MA, USA) at room temperature for 30 min on medium speed to dissociate the cells from the gill lamellae. The dissociated cells and any remaining gill tissue were filtered through a 100 µm cell culture filter into a fresh tube. The filter was washed several times with fresh L-15 media to extract all dissociated cells. The sample was centrifuged for 8 min at 189*g* on a Sorvall Legend XFR centrifuge at 4°C. The supernatant was removed and discarded, and the pellet was re-suspended in 5 mL of distilled water for 30 s to achieve red blood cell lysis (Shahsavarani et al., 2006). Immediately after the 30 s lysis period, 15 mL of L-15 media were added to the cell suspension and mixed by shaking. The cells were then centrifuged for 8 min at 189*g*, the supernatant was discarded, and the cells were re-suspended in 1.5 mL of L-15 media and transferred to a 2 mL microcentrifuge tube.

Comparison of the final protocol described above with the protocol reported by Shahsavarani et al. (2006) reveals two significant differences, the use of EDTA rather than trypsin-EDTA for cell dissociation, and the use of L-15 media rather than phosphate-buffered saline (PBS) for cell suspension. Whereas Shahsavarani et al. (2006) utilized trypsin-EDTA (0.25% trypsin, 1·mmol·l^{-1} EDTA) to achieve cell dissociation, the final protocol developed in the present study used 200 µL of 0.5 M EDTA. This approach was adopted after testing both protocols on separate preparations and assessing cell viability using the trypan blue exclusion method. Note that when tissue was incubated with trypsin, it was filtered into ‘stop’ solution, 10% foetal bovine serum in PBS, to halt the enzymatic digestion by trypsin (Shahsavarani et al. 2006). Following re-suspension of the final cell pellet, 100 µL of cell suspension was mixed with 400 µL of 0.4% trypan blue solution (ThermoFisher Scientific, Ottawa, ON, Canada) and

the number of trypan-blue containing cells relative to the total number of cells in an aliquot was determined using a haemocytometer.

During the initial stages of protocol development, PBS was used for dissociation, following red blood cell lysis, and during labelling and FACS (see below). However, low cell yields during FACS, suggested that an alternative medium was needed, and therefore L-15 media, which provides nutrients to dissociated cells for better survival was assessed. Following increased cell yields, L-15 media was adopted.

2.3 Cell labelling

Biotin-conjugated PNA (20 µL; Sigma-Aldrich, Oakville, ON, Canada) was added to each 1.5 mL suspension of dissociated trout gill cells to label PNA^+ ionocytes, and incubated on a rocking shaker (Reliable Scientific) at 4˚C for 30 min. The 1:76 dilution was decided through flow cytometry trial as being the volume at which the PNA^+ ionocytes were easily detected by the flow cytometer. The cells were then centrifuged for 2 min at 189*g* at 4°C, the supernatant was discarded and the pellet was re-suspended in 1.5 mL of fresh L-15 media. This washing procedure was repeated twice more. Following the final wash, the cells were once again re-suspended in 1.5 mL of L-15 media and 10 µL of streptavidin conjugated to a 633nm fluorochrome (Sigma-Aldrich, Oakville, ON, Canada) was added to fluorescently label the biotin- conjugated PNA. Again, the cells were incubated on a rocking shaker (Reliable Scientific) at 4˚C for 30 min and then washed three times using 1.5 mL of fresh L-15 media each time. Following the final wash, the cells were re-suspended in 3 mL of L-15 media and were filtered through a 100 µm cell culture filter (ThermoFisher Scientific) followed by a 40 µm filter (ThermoFisher Scientific) to eliminate any clumps of cells that had formed. The cell suspension

was then diluted to a total volume of 5 mL using L-15 media and kept on ice until it was used for flow cytometry or FACS.

2.4 Flow cytometry and FACS

Flow cytometry was carried out on Beckman Coulter Gallios Flow Cytometer. A 647nm laser was used to detect the PNA staining, while 488nm lasers were used to detect size and granularity. The voltage was adjusted to 425V because this setting yielded the most prominent and separate peaks for cell populations that were tested. Experiments were carried out at room temperature, because the flow cytometer did not have a capacity for temperature control. For flow cytometry experiments to establish gates and assess cell viability, dissociated cell suspensions were generated and labelled as described above, with the following modifications. An initial experiment used a dissociated cell suspension that was divided into two aliquots, one of which was labelled as described above while the other was used without labelling, to establish the relative background fluorescence of dissociated gill cells. Also, the Zombie Aqua™ viability dye (BioLegend, San Diego, California, USA) was used in several trials to assess cell viability relative to PNA labelling. In these experiments, 10 µL of the Zombie Aqua™ viability dye was added together with the streptavidin-conjugated fluorophore.

Cell sorting for methods development, as well as for the proof-of-principle experiment, was carried out using one of two Beckman Coulter MoFloAstrios EQ Cell Sorters, that in RGN and that in D'Iorio Hall at the University of Ottawa. Cell sorting was carried out using four lasers: a side scatter laser to detect granularity, a forward scatter laser to detect the size of the particles, a second forward scatter laser at an angle different from first to monitor and discard cell clumps, and a 647nm laser for the detection of fluorescence from the biotin-conjugated

PNA/streptavidin-633nm fluorochrome versus the 'negative' or unlabelled cell fraction. Sorting took place immediately following cell dissociation, with the temperature of the sorter kept at 4°C. On average, sorting of a single sample of 5 mL volume required 2-3 h, depending on whether clumping occurred in the sample requiring re-filtering samples through a 40 µm filter (ThermoFisher Scientific) and/or whether the cell sorter had to be cleaned.

The PNA^+ and negative cell fractions were collected into 500 µL of L-15 media for further analysis with flow cytometry or immunohistochemistry, or into a 500 µL solution of lysis buffer (450 µL; QIAGEN RNeasy Kit, QIAGEN, Toronto, ON, Canada) containing RNAlater® solution (50 µL; ThermoFisher Scientific) for cell lysis and subsequent RNA extraction. These protocols were adopted after experiments to identify approaches that yielded sufficient RNA and RNA of sufficient quality for subsequent real-time RT-PCR. In initial experiments, dissociated rainbow trout gill cells were sorted by FACS into 500 µL of L-15 media. When the entire sample had been collected, the suspension was centrifuged at 300*g* for 5 min to form a pellet. The supernatant was discarded and the cell pellet was re-suspended in lysis buffer for RNA extraction (as described below). Analysis of this RNA using a NanoDrop® ND-1000 UV-Vis Spectrophotometer (ThermoFisher Scientific) revealed RNA yields that were too low for subsequent experiments. To address this issue, an alternative method was tested in which cells were collected directly into lysis buffer containing RNAlater™ (as described above), to shorten the time between cell sorting and cell lysis, and to eliminate a centrifugation step. Higher amounts of RNA were extracted, and this approach was therefore used for all other experiments.

2.5 Immunocytochemistry

To assess cells isolated by FACS, PNA^+ cells were collected into 500 µL of L-15 media. The collected cells were centrifuged at 300*g* for 5 min, the supernatant was discarded, and the pellet was re-suspended in 10 µL of Vectashield Antifade mounting medium (Vector Laboratories, Burlington, ON, Canada) containing 4′,6′-diamidino- 2-phenylindole (DAPI) for the visualization of nuclei. Aliquots (2 µL) of cell suspension were plated onto electrostatically charged slides (FisherbrandSuperFrost Plus, ThermoFisher Scientific), to a total of 5 slides per sample. The cells were viewed by confocal microscopy (Nikon A1RsiMP, Ottawa, ON, Canada)**.**

2.6 Proof-of-principle experiment – transcript abundance in response to metabolic alkalosis

Rainbow trout were exposed to control conditions or to metabolic alkalosis achieved by 72 h of hypercapnic exposure (1% CO_2) followed by 6 h of normocapnic recovery, as described by Brannen and Gilmour (2018). Owing to constraints associated with FACS, only two fish could be tested in a day, and therefore each trial consisted of one control fish and one fish exposed to metabolic alkalosis. Rainbow trout were randomly allocated to the control or metabolic alkalosis treatment group (N = 7 for each group) and were transferred to individual 6 L experimental chambers for a 24 h acclimation period. Fish were held in 6 L of 13˚C water in a static system. Water temperature was maintained by placing the experimental chambers in a larger tank supplied with flowing 13˚C water. At least 50% of the water volume was changed every 12 h with minimal disturbance of the fish. The experimental chambers were aerated during the acclimation period. The fish in the metabolic alkalosis treatment group was then exposed to hypercapnia for 72 h by aerating the water with a mixture of 1% CO_2 in air achieved using mass flow controllers (SmartTrak 100 series, Sierra Instruments, SRB Controls, Monterey, California,

USA). During this period of hypercapnia, water was equilibrated with the same mixture of 1% CO_2 in air prior to being used to refresh the water in the experimental chamber. After 72 h, aeration to trout in the treatment group was returned to air for 6 h of recovery. Both control and treatment trout were euthanized by a cephalic blow and gill tissue was collected.

Gill tissue was processed as described above to achieve a suspension of dissociated cells, and the suspension was labelled with PNA and subjected to FACS as described above to isolate the PNA^+ ionocyte and negative fractions. Cells were collected into lysis buffer containing RNAlater® as described above, and RNA was extracted from the sample using the RNeasy kit (QIAGEN), as described by the manufacturer. The extracted RNA was quantified (NanoDrop® ND-1000 UV-Vis Spectrophotometer; ThermoFisher Scientific) and 500 ng of total RNA was used for cDNA synthesis (QuantiTect Reverse Transcription Kit; QIAGEN), used according to the manufacturer's protocol. A "no reverse transcriptase" (RT) control sample was used in this experiment to confirm that genomic DNA had been eliminated. This control sample was generated as above, except that reverse transcriptase was not added to the sample during cDNA synthesis.

Primers for the genes of interest, *cac*, *nka*, *nhe2* and *nhe3*, as well as the housekeeping gene, *ef1α*, were identified from the literature (Table 2.1). To test the *cac* and *nka* primers as well as the quality of the RNA extracted from isolated cells and used for cDNA synthesis during the methods development stage of this project, conventional PCR was carried out for 20-40 cycles ($S1000^{TM}$ Thermal Cycler, BioRad, USA), at 5 cycle increments, and the PCR products were examined by gel electrophoresis. Gel electrophoresis was carried out on a 1% agarose gel, at 60 V for 1 hour. All real-time RT-PCR was carried out on CFX96 Real-Time PCR System (C-1000 Touch Thermal Cycler; BioRad, USA). Standard curves using 5X dilutions were constructed for

each gene (Table 2.1) from pooled samples of PNA^+ ionocyte fractions generated during the final stage of methods development, when protocols had been optimized. Each reaction consisted of 5 µL of master mix (SsoFast™ EvaGreen® Supermix, BioRad, Singapore), 0.4 µL each of forward and reverse primers, 0.2 µL of water and 4 µL of cDNA template at 1:625 dilution, making 10 µL of total reaction volume. For each assay, cycling parameters consisted of a 3 min initial denaturation step at 95°C followed by 40 cycles consisting of 95°C for 30 s for denaturation, 56°C for 30 s for annealing, and 72°C for 1 min for extension, and ending with 10 min at 72°C for final extension. All samples were assayed in triplicate. Every plate included an inter-plate calibrator as well as no template controls (where cDNA was replaced with H_2O) and no RT controls. The mRNA abundance of PNA^+ ionocyte and negative fractions in each treatment group was calculated relative to the mRNA abundance of the negative fraction from control fish. Relative abundance for each sample was calculated using the delta-delta Ct method (Livak and Schmittgen, 2001), and normalized to the mRNA abundance of the reference gene *ef1α*, as this gene remained constant among all groups and samples used in the experiment. The statistical significance of differences in relative mRNA abundance was assessed using two-way analysis of variance (ANOVA) with treatment group and cell fraction as the two factors, and a fiducial limit of significance of 0.05. When significant differences were detected, *post hoc* analysis was conducted using the Holm-Sidak test. SigmaPlot v12.5 (Systat Software) was used to accomplish all statistical analysis. Data, that did not meet the assumption of normality using the Shapiro-Wilk test were log10 transformed to meetcthe assumptions of normality. Data are presented as mean values ± 1 standard error of the mean (s.e.m.)

Table 2.1. Primer information for the genes of interest.

Gene	Primer pair sequences (5' to 3')	R^2	Efficiency (%)	GenBank #	Reference
cac	F - 5' CAGTCTCCCATTGACATCGTA 3'	0.993	101.1	NM_001124220.1	Grosell et al., 2007
	R - 5' CGTTGTCGTGGTGTAGGT 3'				
nka	F - 5' GGCCGGCGAGTCCAATCAT 3'	0.991	95.1	NM_001124461.1	Gallagher et al., 2013
	R - 5' GAGCAGCTGTCCAGGATCCT 3'				
nhe2	F - 5' TGTGCCCTGACCATGAAGTA 3'	0.990	101.6	NM_001130994.1	Ivanis et al., 2008
	R - 5' CCCAGTTCCACTCGTGTTCT 3'				
nhe3	F - 5' AGAGCAGCCGTGACAGAACT 3'	0.970	114.0	NM_001160482.1	Ivanis et al., 2008
	R - 5' AACCAGCACAACCACCTCTC 3'				
ef1α	F - 5' CATTGACAAGAGAACCATTGA 3'	0.990	99.5	NM_001124339.1	Sànchez et al., 2011
	R - 5' CCTTCAGCTTGTCCAGCAC 3'				

Chapter 3 RESULTS

3.1 Methods development and validation experiments

In initial experiments to develop a suspension of dissociated trout gill cells that was suitable for flow cytometry and FACS, the methods developed by Goss et al. (2001) on PNA staining, Galvez et al. (2002), and Shahsavarani et al. (2006) were used. This approach utilized enzymatic digestion with trypsin to dissociate cells. Owing to concerns about the yield of viable cells with trypsin, the Ca^{2+} chelating agent EDTA was also tested as a means of achieving cell dissociation. Following two trials with each approach, the cell viabilities (based on trypan blue exclusion) for trypsin digestion were found to be 55.7% and 53.5% whereas that for cells dissociated by EDTA treatment were 73.8% and 70.8%. Thus, subsequent attempts utilized EDTA. A second problem that was encountered was the tendency for cells to aggregate into large clumps. This problem was largely overcome by elimination of RBCs and the use of Ca^{2+}-free solutions.

As in the work of Goss and colleagues (Goss et al., 2001; Galvez et al., 2002; Shahsavarani et al., 2006), the present study used PNA to identify and isolate PNA^+ ionocytes in suspensions of dissociated gill cells. Flow cytometry carried out on a cell suspension that was split into two aliquots, one of which was incubated with PNA conjugated to biotin followed by streptavidin conjugated to a 633nm fluorophore, revealed that a signal associated with fluorescence at the expected wavelength of 647nm was detected only in the PNA-incubated aliquot (Fig. 3.1A, C). Based on the expected size (~10 µm) and granularity of live mammalian cells studied in other FACS experiments, the anticipated population of live PNA^+ cells was estimated (Fig. 3.1D). Subsequent efforts focused on identifying live cells within the total population of PNA^+ cells (and likely debris) using a Zombie^{TM} Cell Viability Dye. Dead cells

and cellular debris take up more Zombie stain than live cells, where the stain only binds to surface proteins rather than penetrating to the interior of the cell as it does in a dead cell, and therefore flow cytometry on a Zombie-stained population yields two peaks for fluorescence at different intensities, which together with the peak for PNA-linked fluorescence, allows the population of live PNA^+ cells to be identified (Fig. 3.2). In the example presented in Fig. 3.2, 48.8% of the cells in the population were identified as live cells and 9.5% of cells in the population were identified as live PNA^+ cells. Over two experiments, 47.9% of cells on average were live and 8.9% were both alive and PNA^+.

These initial experiments using flow cytometry suggested that PNA-biotin/streptavidin-fluorophore was suitable as a cell marker for isolation of PNA^+ ionocytes by FACS, and trials using FACS therefore were commenced. However, initial attempts (7 in total) did not yield sufficient cells for experiments on the isolated cells, with only 50k-100k PNA^+ cells being obtained. Following five trials in which time and temperature were systematically manipulated, the yield of PNA^+ cells was raised to 200k-300k, which was still deemed to be insufficient for reliable RNA extraction. Next, a switch was made from holding cells in PBS prior to and during cell sorting, to using Ca^{2+}-free L-15 media. This change led to a substantial increase in PNA^+ cell yield, with 600k-800k cells being obtained routinely, and during certain trials, up to a million PNA^+ ionocytes being obtained. At this point, the quality of the PNA^+ cell fraction was examined by assessing purity using flow cytometry and via confocal microscopy. Flow cytometry revealed that 92.2% of the cells in a PNA^+ cell fraction obtained using FACS were indeed PNA-positive (Fig. 3.3). Aliquots of the PNA^+ cell fractions obtained from several different cell sorting trials were mounted on glass slides using mounting medium containing DAPI for visualization of nuclei. Confocal fluorescence microscopy carried out on these aliquots revealed few cells that

were not PNA-positive (Fig. 3.4). Cell counts carried out on two independent samples yielded 68 PNA^+ cells with 3 that did not show PNA-related immunofluorescence in the first sample, and 82 PNA^+ cells with 7 negative cells in the second sample. These cell counts indicate that the mean purity was 94% over the two samples.

The final step in developing an appropriate protocol to obtain isolated PNA^+ ionocytes for assessment of transcript abundance by real-time RT-PCR involved assessing different methods for cell collection and RNA extraction. Various approaches were tested, including sorting cells directly into lysis buffer; sorting cells into PBS or L-15 media, pelleting the cells by centrifugation and then lysing the cell pellet for RNA extraction; and collecting the cell fraction into aliquots that were lysed as collected. However, all of these methods produced low and variable RNA yields. Consistent RNA yields of 50-60 ng μL^{-1} were finally obtained by sorting cells into lysis buffer containing RNAlater®. The success of this approach was apparent from PCR trials in which *cac* and *nka* transcripts were amplified from cDNA that was synthesized from RNA extracted from isolated PNA^+ ionocyte populations (Fig. 3.5).

3.2 Assessment of transcript abundance in PNA^+ ionocyte fractions

Relative transcript abundances of *cac*, *nka*, *nhe2* and *nhe3* were assessed by real-time RT-PCR carried out on PNA^+ ionocytes as well as the non-PNA^+ cell fraction (negative) isolated from control rainbow trout and trout that were exposed to a metabolic alkalosis via recovery from 72 h of hypercapnia. Relative transcript abundance of *cac* was significantly elevated in PNA^+ ionocytes of alkalotic trout relative to all other groups (Fig. 3.6A; 2-way ANOVA carried out on log10-transformed data, $P = 0.001$ for the effect of treatment group, $P = 0.001$ for the effect of cell population, and $P = 0.002$ for treatment x cell population). The relative transcript

abundance of *nka* was significantly elevated in PNA^+ ionocytes relative to the negative fraction, and to a greater extent in PNA^+ ionocytes from alkalotic relative to control trout (Fig. 3.6B; 2-way ANOVA carried out on log10-transformed data, $P = 0.001$ for the effect of treatment group, $P = 0.001$ for the effect of cell population, and $P = 0.001$ for treatment x cell population). For both *nhe2* and *nhe3*, relative transcript abundances were significantly elevated in PNA^+ ionocytes relative to the negative cell fraction, but with no significant effect of exposure to alkalosis in either cell fraction (Fig. 3.7; 2-way ANOVA, $P = 0.228$ for the effect of treatment group, $P = 0.03$ for the effect of cell population, and $P = 0.396$ for treatment x cell population for panel A, and $P = 0.836$, 0.001, and 0.414, respectively, for panel B).

Figure 3.1. Representative flow cytometer readouts presenting flow cytometry assessment of peanut lectin agglutinin (PNA) staining on a suspension of dissociated gill cells from rainbow trout (*Oncorhynchus mykiss*). A dissociated gill cell population was divided into two samples, one of which was incubated with PNA. Panels A and B present representative figures collected for the unstained sample. Panel A shows that the unstained cells did not exhibit fluorescence, and panel B presents the side (SS) and forward scatter (FS) data, representing granularity and size, respectively, for the population of cells in this sample. Panels C and D present data collected for the gill cell sample that was incubated with PNA. Panel C shows that 39.6% of the cell population exhibited fluorescence associated with PNA labelling. Panel D presents the side and forward scatter information for the population of cells, with PNA-labelled cells and particles indicated in red. Because the sample contained both live and dead cells as well as cellular debris that could have bound PNA, it is not possible to pinpoint the true PNA^+ cell population without a secondary marker for viability. The circle in Panel D suggests where a population of live, PNA-labelled cells would be expected to be found based on the size and granularity of the cells that were counted.

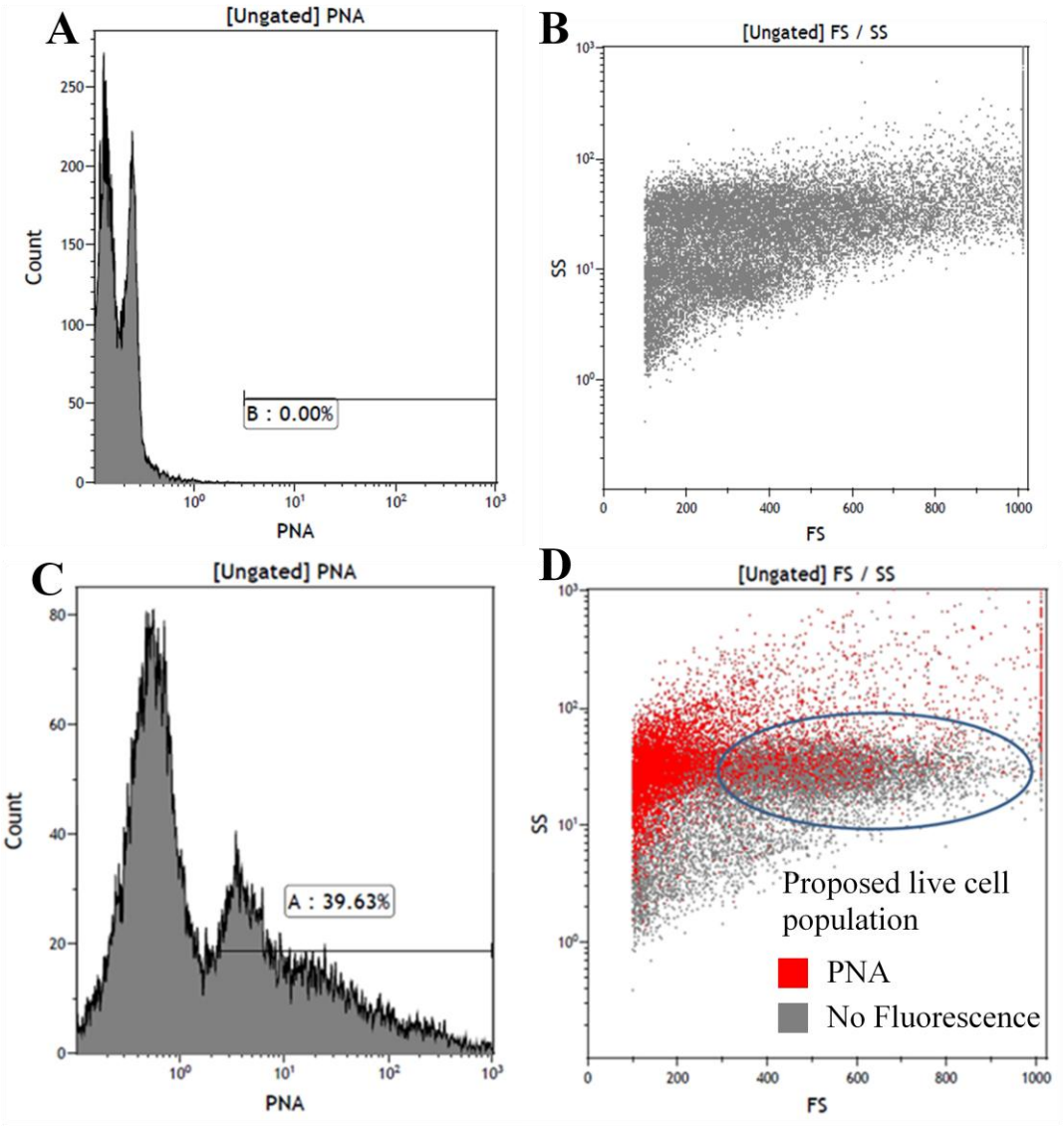
A
[Ungated] PNA
Count
PNA
B : 0.00%
B
[Ungated] FS / SS
SS
FS
C
[Ungated] PNA
Count
PNA
A : 39.63%
D
[Ungated] FS / SS
SS
FS
Proposed live cell population
PNA
No Fluorescence

Figure 3.2. Representative flow cytometer readouts presenting the flow cytometry assessment of a suspension of dissociated gill cells from rainbow trout (*Oncorhynchus mykiss*) that were labelled with peanut lectin agglutinin (PNA) and Zombie^{TM} cell Viability Dye. Panel A shows fluorescence detected for PNA-labelled versus unlabelled cells, with 24.0% of the cells exhibiting fluorescence associated with PNA labelling. Panel B presents fluorescence associated with Zombie staining, with the peak for live cells, which take up less stain, accounting for 48.8% of the cell population. In panel C, side (SS) and forward scatter (FS) data, representing granularity and size, respectively, are presented for the entire cell population with live cells indicated in red, dead cells and debris indicated in green, and cells or particles that exhibit co-labelling of PNA indicated in blue. In panel D, the population of dead cells and debris, as well as live non-PNA^{+} cells were removed, leaving the population of live, PNA^{+}-labelled cells which represented 9.5% of the cells found in the original sample.

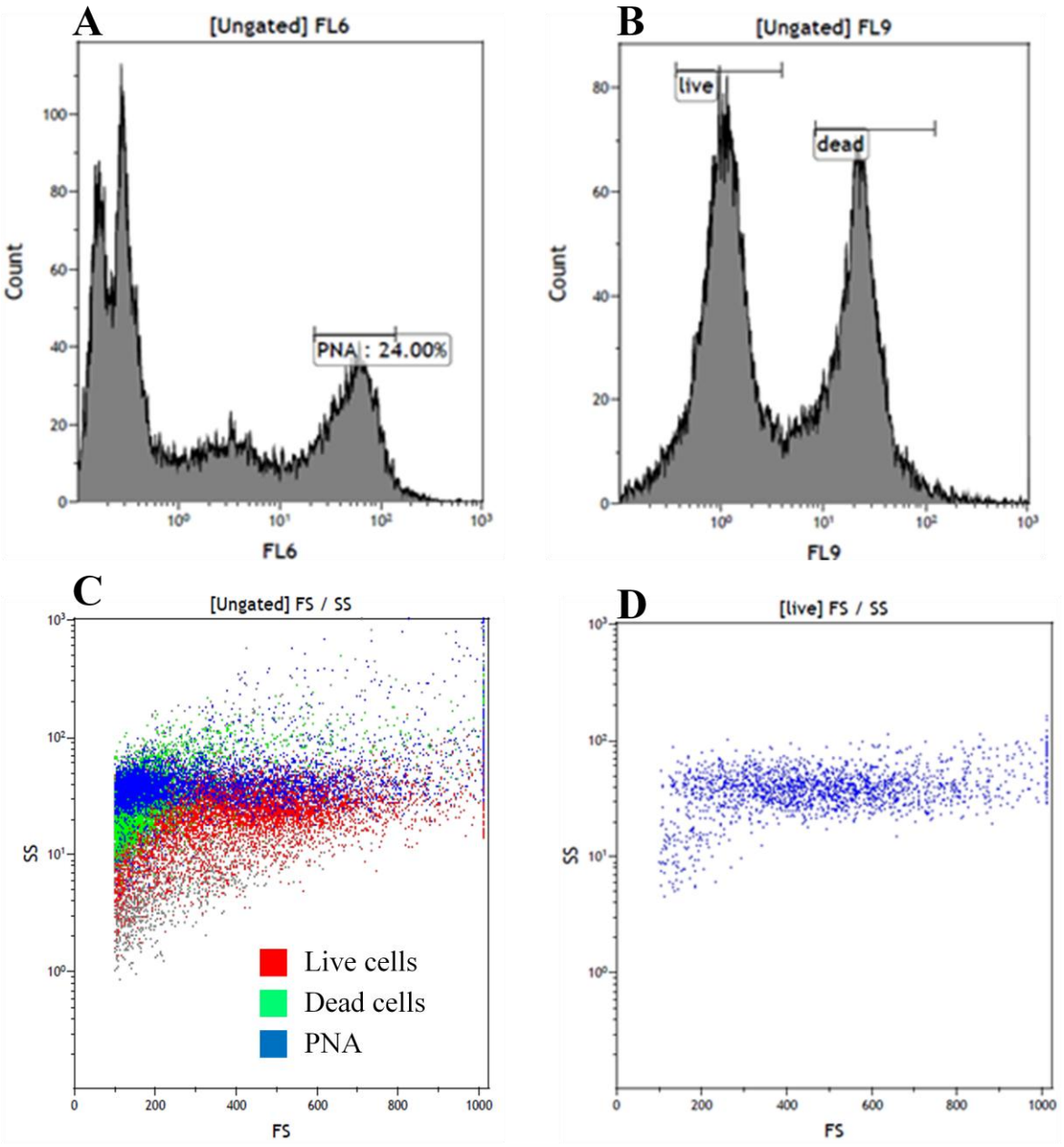
A
[Ungated] FL6
Count
FL6
PNA : 24.00%
B
[Ungated] FL9
Count
FL9
live
dead
C
[Ungated] FS / SS
SS
FS
Live cells
Dead cells
PNA
D
[live] FS / SS
SS
FS

Figure 3.3. Representative flow cytometer readouts illustrating the purity of a peanut lectin agglutinin-positive (PNA^+) cell population isolated from a rainbow trout (*Oncorhynchus mykiss*) dissociated gill cell suspension through fluorescence-activated cell sorting (FACS). Flow cytometry output for a population of PNA^+ cells generated by FACS that was re-run on the FACS immediately after collection. Panel A is a dot plot representing all events in the sorted sample with side scatter on the x-axis and fluorescence on the y-axis. The dots within the gate represent all PNA^+ ionocytes in the sample, while all dots outside the gate are the impurities. Panel B is another variation of the data presented in panel A, with fluorescence now plotted on x-axis and total count of events plotted on y-axis. The gate once again represents all PNA^+ ionocytes in the sample, while events outside the gate represent impurities. Based on this representative sample, 92.2% of the cells in the sorted sample were PNA^+, i.e. the purity of the PNA^+ cell population obtained through FACS was 92.2%.

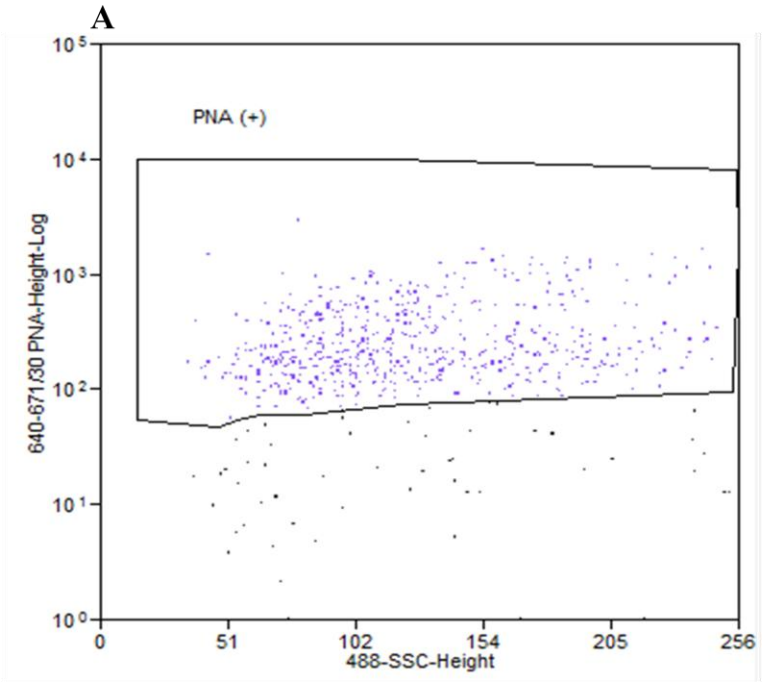

C

Region	Count	% Hist	% All
Total	696	100.00	84.67
PNA (+)	642	92.24	78.10

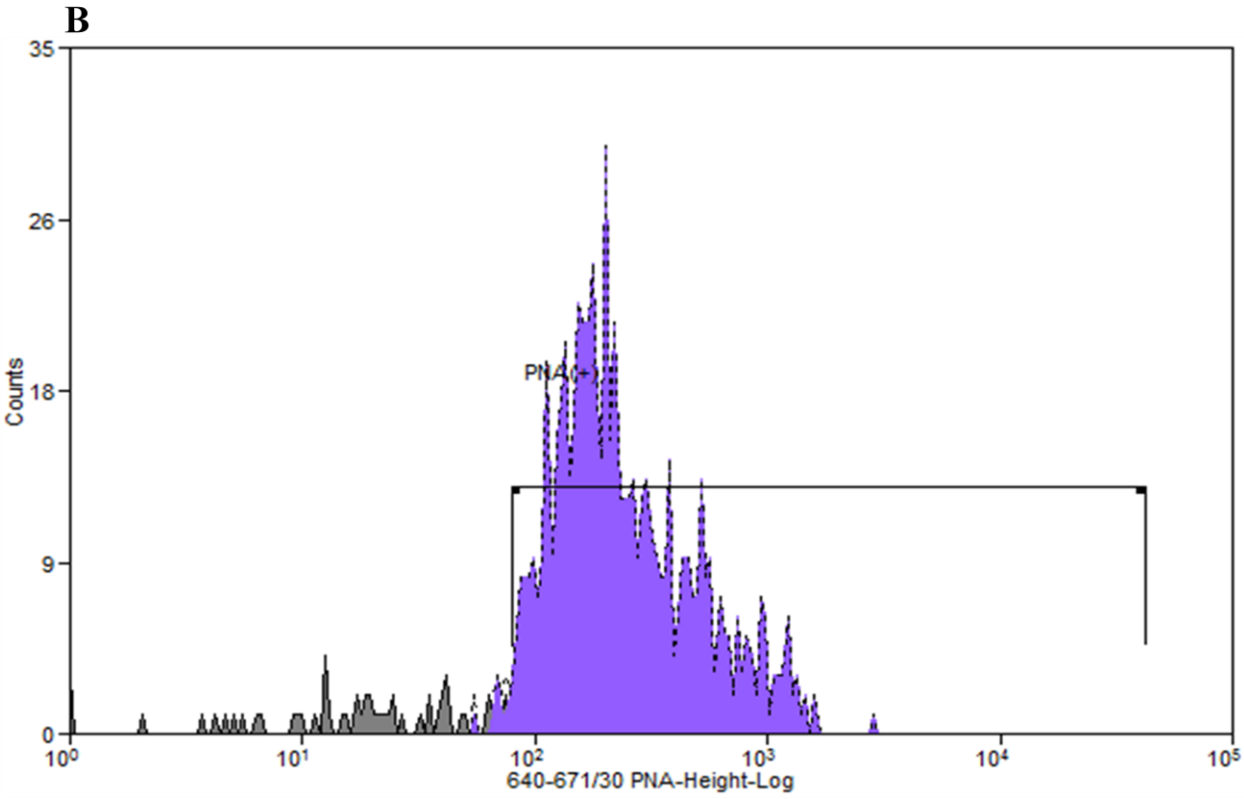

Figure 3.4. Representative micrographs (A-E) of peanut lectin agglutinin-positive (PNA^+) cells isolated from a suspension of dissociated gill cells of rainbow trout (*Oncorhynchus mykiss*) by fluorescence-activated cell sorting (FACS). A representative image of a cell that was sorted into the PNA^+ fraction, but was not a PNA^+ ionocyte, i.e. a 'negative' cell and impurity, is also presented (F). Each row of images presents (red) fluorescence associated with PNA in the first image, and 4',6-diamidino-2-phenylindole (DAPI) (blue) in the second image; an overlay of PNA and DAPI is presented in the third image of each row, with co-localization of DAPI and PNA indicated in pink. Scale bar = 10 µm.

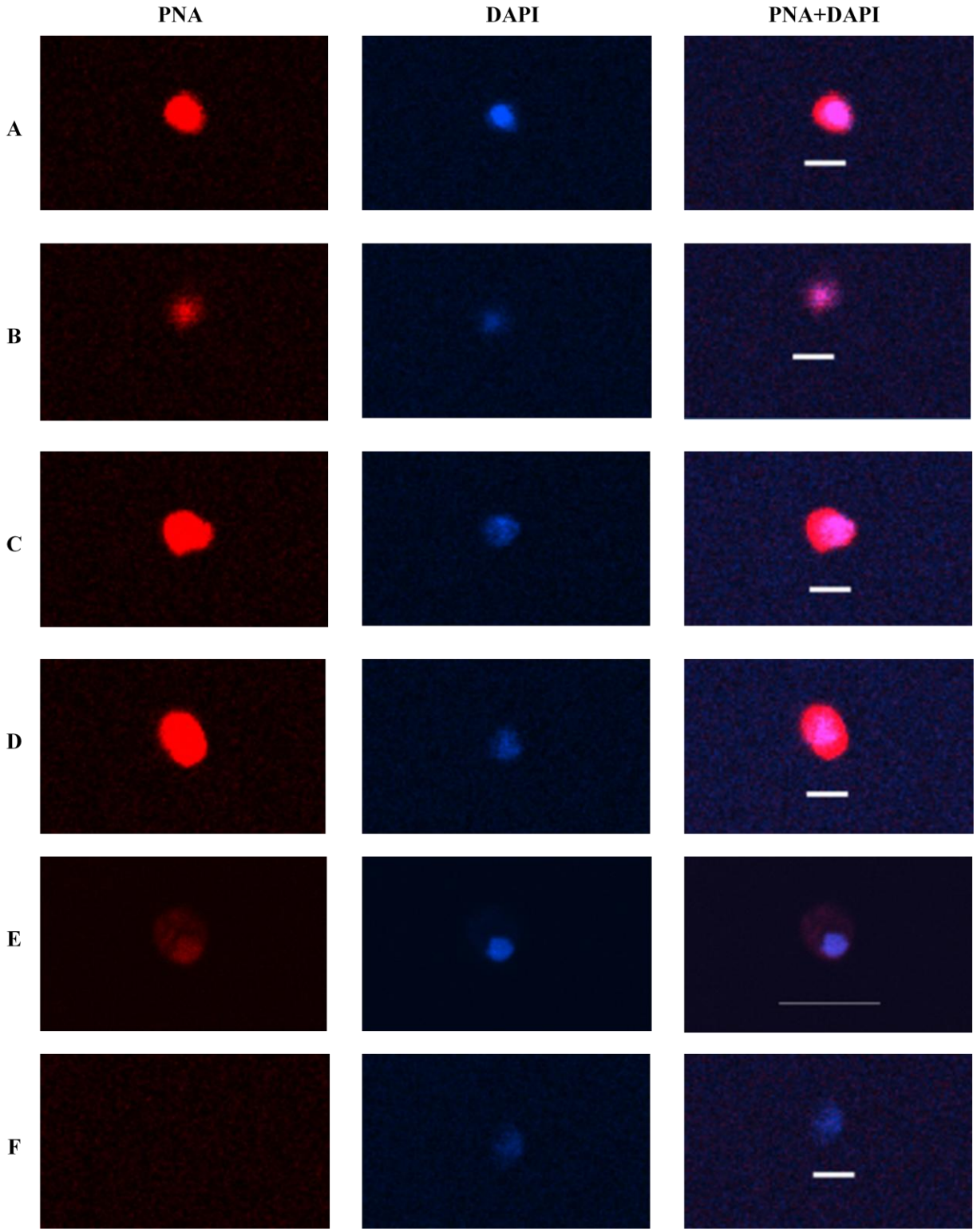
PNA
DAPI
PNA+DAPI
A
B
C
D
E
F

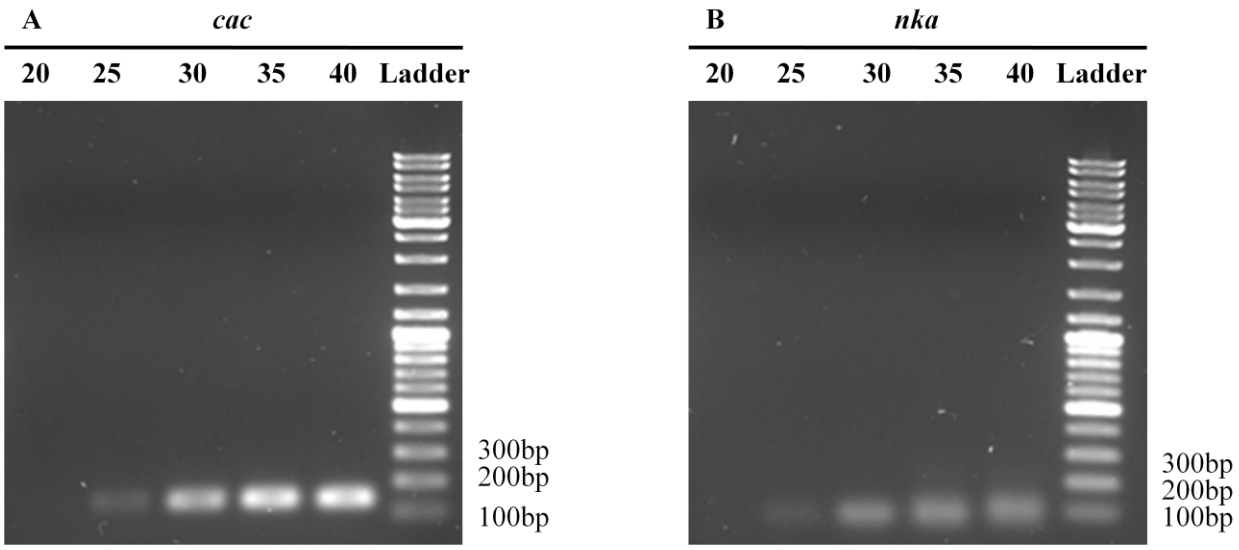

Figure 3.5. Representative images of PCR products for trout cytosolic carbonic anhydrase (*cac*; A) and Na^+, K^+-ATPase (*nka*; B) carried out on cDNA synthesized from RNA extracted from PNA^+ ionocytes. The numbers above the lanes represent the number of cycles over which PCR was carried out. For both genes, a product is visible from 25 cycles of PCR, with the PCR product for *cac* around 150bp and that for *nka* approximately 100bp; these were the expected product sizes.

Figure 3.6. Relative mRNA abundances of cytosolic carbonic anhydrase (*cac*; A), and Na^+, K^+-ATPase (*nka*; B) in gill cell populations obtained from rainbow trout (*Oncorhynchus mykiss*) that were exposed to control conditions or to recovery from hypercapnia (recovery; see text for treatment details). The gill cell populations were peanut lectin agglutinin-positive (PNA^+) cells and cells that were not PNA^+ (negative) obtained from a suspension of dissociated gill cells by fluorescence-activated cell sorting. Values are means + s.e.m. with $N = 7$ in all groups, and transcript abundance was expressed relative to the negative cells from the control treatment group, using elongation factor 1 alpha as a housekeeping gene. Groups that share a letter are not significantly different from one another (2-way ANOVA, $P = 0.001$ for the effect of treatment, 0.001 for the effect of cell population, and 0.002 for treatment x population in panel A, and 0.001, 0.001 and 0.001, respectively, in panel B).

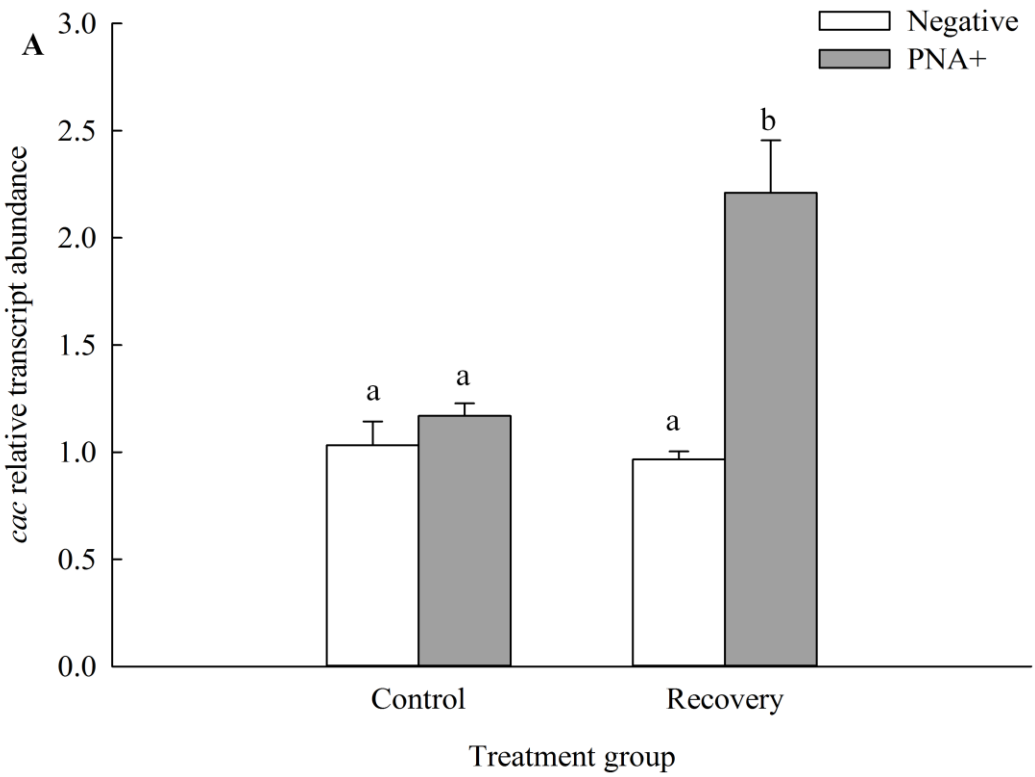
A
Negative
PNA+
3.0
2.5
2.0
1.5
1.0
0.5
0.0
cac relative transcript abundance
a
a
a
b
Control
Recovery
Treatment group

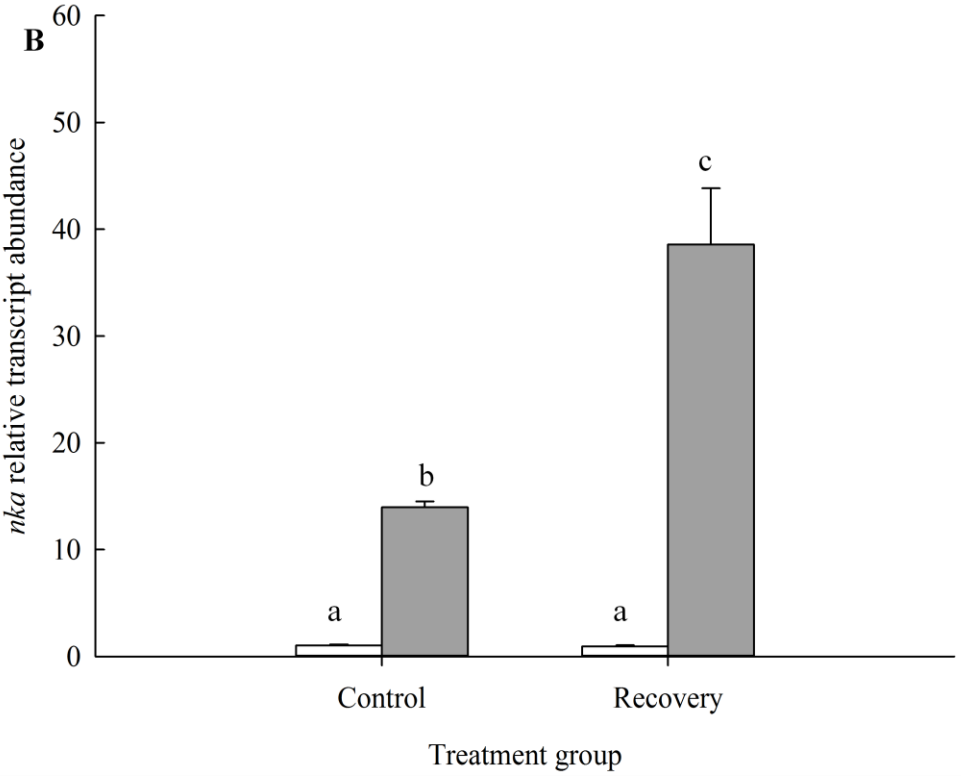
B
60
50
40
30
20
10
0
nka relative transcript abundance
a
b
a
c
Control
Recovery
Treatment group

Figure 3.7. Relative transcript abundances of Na^+/H^+ exchanger isoform 2 (*nhe2*; A), and *nhe3* (B) in gill cell populations obtained from rainbow trout (*Oncorhynchus mykiss*) that were exposed to control conditions or to recovery from hypercapnia (recovery; see text for treatment details). The gill cell populations were peanut lectin agglutinin-positive (PNA^+) cells and cells that were not PNA^+ (negative) obtained from a suspension of dissociated gill cells by fluorescence-activated cell sorting. Values are means + s.e.m. with $N = 7$ in all groups, and transcript abundance was expressed relative to the negative cells from the control treatment group, using elongation factor 1 alpha as a housekeeping gene. Groups that share a letter are not significantly different from one another (2-way ANOVA, $P = 0.228$ for the effect of treatment group, 0.03 for the effect of cell population, and 0.396 for treatment x population in panel A, and 0.836, 0.001 and 0.414, respectively, for panel B).

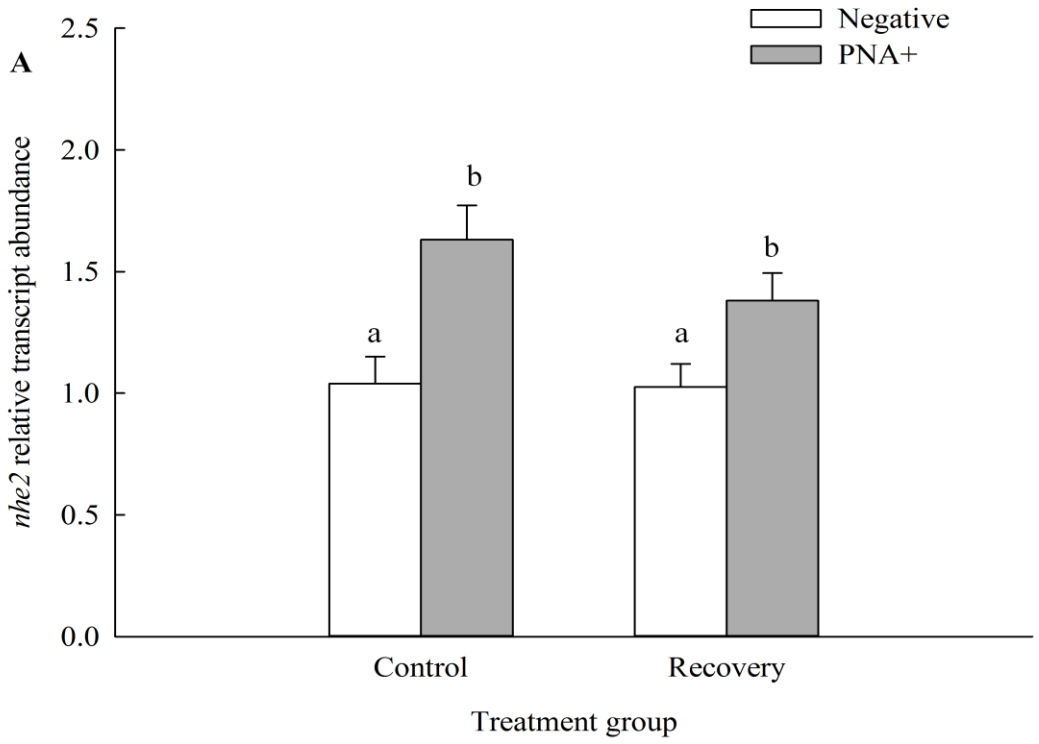
A
Negative
PNA+
2.5
2.0
1.5
1.0
0.5
0.0
nhe2 relative transcript abundance
a
b
a
b
Control
Recovery
Treatment group

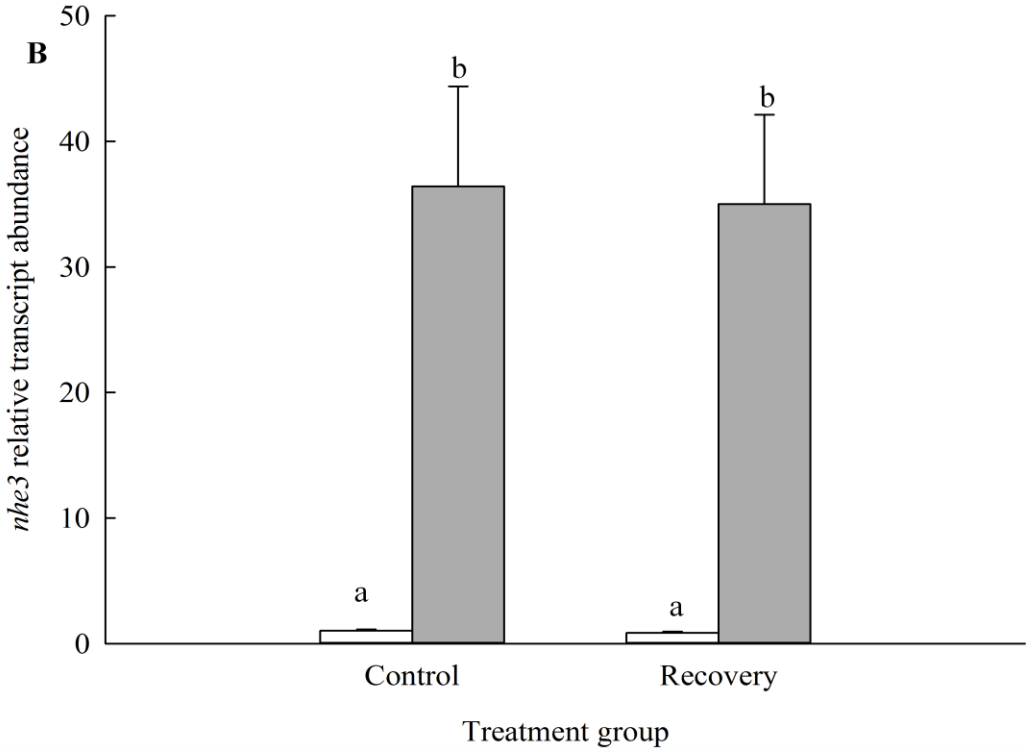
B
50
40
30
20
10
0
nhe3 relative transcript abundance
a
b
a
b
Control
Recovery
Treatment group

Chapter 4 DISCUSSION

This study attempted to answer the question of whether transcriptional regulation of *cac* occurs in PNA^+ cells of the trout gill epithelium in response to metabolic alkalosis. To address this question, the study developed and employed an experimental approach that allowed isolation and assessment of PNA^+ cells specifically, i.e. the use of FACS with PNA as the marker for the cell type of interest. Support for the hypothesis that transcriptional regulation of *cac* occurs in an ionocyte-specific fashion in response to acid-base disturbances was obtained in that *cac* mRNA abundance increased significantly in PNA^+ cells following exposure of trout to metabolic alkalosis. These data provide support for the hypothesis that PNA^+ cells are a base-secreting ionocyte within the trout gill epithelium.

Recent research on acid-base and ion regulation in teleost fish led to the discovery of multiple ionocyte types as well as models of how each ionocyte type would be expected to function in ion uptake and acid-base regulation (Evans et al., 2005; Hwang et al., 2011; Gilmour, 2012; Kumai and Perry, 2012; Dymowska et al., 2012). For example, the discovery of PNA^+ versus PNA^- ionocytes in the gill epithelium of rainbow trout (Goss et al., 2001) steered researchers to develop a model of the PNA^+ cell as a base-secreting cell for Cl^- uptake and the PNA^- cell as an acid-secreting cell for Na^+ uptake. This model, particularly for the PNA^- cell, has been supported by empirical data (Galvez et al., 2002; Reid et al., 2003; Goss et al., 2011; Brannen and Gilmour, 2018) but the studies yielding these empirical data have also generated unexpected results. In particular, Brannen and Gilmour (2018) reported that CAc was rarely detected by immunohistochemistry in PNA^+ cells under control conditions (it was detected in only 5% of PNA^+ cells), with the number of CAc-positive, PNA^+ ionocytes increasing markedly in trout experiencing an alkalosis. These findings contrasted with the expected need for CAc in

both ionocyte types, to catalyze the hydration of CO_2 to generate acid-base equivalents (Gilmour and Perry, 2009; Goss et al., 2011). To further investigate these findings, which raised new questions about the function of PNA^+ cells under control conditions and their response to alkalosis, an approach that allows isolation of the cell type of interest was needed. Goss and colleagues (Goss et al., 2001; Galvez et al., 2002) developed a cell isolation approach for the rainbow trout gill epithelium that utilized separation of cell types along a Percoll gradient followed by magnetic cell separation (MACS) using PNA conjugated to fluorescein isothiocyanate (FITC) and an antibody against FITC coupled to iron particles to identify and isolate PNA^+ cells. With this approach, Galvez et al. (2002) reported >95% purity within the population of isolated PNA^+ ionocytes, but the method was difficult to replicate and as such has not been widely adopted. The present study aimed to develop an alternative approach for ionocyte isolation based on FACS.

4.1 Methods development and validation

The use of FACS requires that the cells of interest be labelled and present within a suspension of dissociated cells. Thus, an initial focus of the study was the generation of an appropriate cell suspension from rainbow trout gill tissue. The requirements for the cell suspension included high cell viability, that the cells remain dissociated without clumping for the several hour process of cell sorting, and that the population of the cells of interest be labelled reliably. The starting point for development of an appropriate, reliable cell dissociation protocol was the work of Shahsavarani et al. (2006), in which trypsin-EDTA in PBS was used to dissociate trout gill cells, with dissociated cells being held in PBS. Earlier work also utilized enzymatic digestion, with type 1A collagenase in Cortland's saline being used by Galvez and colleagues (2002) in the preparation of gill cells for MACS. The trypsin-EDTA protocol was

modified with the goal of increasing the yield of viable cells and the period of time over which the cells remained viable. The first change was a switch from PBS to Ca^{2+}-free L-15 media, because media provides not only buffers for pH control, but also amino acids and vitamins that help in maintaining cell viability (Arora, 2013). Second, EDTA on its own rather than trypsin-EDTA was used to promote cell dissociation. The chelating agent EDTA is able to dissociate cells by removing Ca^{2+} from the vicinity of cells, which has the effect of breaking the adherens junctions, a Ca^{2+}-dependent cell-cell attachment (Peracchia, 1977). Studies in mammals reported that both the viability and morphology of dissociated cells were improved by dissociation using EDTA rather than trypsin (Vogl, 1978; Osman and Ruch, 1981). For example, trypsin-dissociated mouse odontoblast cells lost their morphology almost immediately, whereas those dissociated using EDTA retained their native morphology for 15-18 h (Osman and Ruch, 1981). Similarly trypsin was found to force the release of cell-surface glycoproteins from human fibroblasts, whereas cells dissociated with EDTA retained these glycoproteins (Vogel, 1978). In the present study, trout gill cells dissociated using EDTA exhibited higher viability than those dissociated using trypsin, leading to the choice of EDTA as the main dissociation agent.

Goss et al. (2001) first reported that the lectin PNA identified a specific population of cells in the gills of rainbow trout that were deemed to be ionocytes on the basis of the mitochondrial stain MitoTracker®; indeed, PNA^+ ionocytes appeared always to exhibit MitoTracker® staining, suggesting that PNA alone would be sufficient to identify this cell population (Goss et al., 2001; Galvez et al., 2002; Reid et al., 2003). Thus, the present study used PNA conjugated to biotin, with detection by means of streptavidin conjugated to a fluorophore, an approach used in previous studies to identify PNA^+ ionocytes (Ivanis et al., 2008; Brannen and Gilmour, 2018). Biotinylated PNA in combination with streptavidin conjugated to a

fluorochrome was used over PNA conjugated to a fluorochrome for signal amplification and hence better detection. Although the stronger signal obtained is a major advantage of this approach, a disadvantage comes from possibility of non-specific staining if streptavidin binds to endogenous biotin. Unfortunately, an important control was missed in the protocol development stage of the present study; specifically, labelling of a dissociated gill cell population only with streptavidin. In this context it is reassuring that no non-specific staining associated with the detection of endogenous biotin by fluorophore-labelled streptavidin was detected in the immunohistochemistry carried out by Ivanis et al. (2008) or Brannen and Gilmour (2018). Nevertheless, it will be important to test that non-specific binding of streptavidin does not occur in dissociated cell populations. A second advantage of labelling cells with biotinylated PNA is the capacity to work with live cells, which facilitates RNA extraction. In cells fixed with PFA, for example, cross-linking of RNA makes RNA extraction difficult (Evers et al., 2011).

Flow cytometry data provided insight into the success of using PNA^+ labelling to identify and isolate PNA^+ ionocytes. In the original study of PNA as a marker for a specific population of trout ionocytes, Goss et al. (2001) reported that approximately 20% of the cells in the rainbow trout gill epithelium were ionocytes (i.e. migrated to a particular layer in a Percoll gradient that was known to contain primarily mitochondrion-rich cells), with about 40% of these ionocytes being labelled by PNA, placing the PNA^+ ionocyte fraction at about 8%. Using MACS, Galvez et al. (2002) reported a comparable value of 6% PNA^+ ionocytes in the gill epithelium. Similarly, in the present study, flow cytometry revealed the fraction of PNA^+ ionocytes to be ~9%. Equally important was the assessment of the purity of the PNA^+ ionocyte fraction obtained by FACS in the present study. Galvez et al. (2002) reported that using Percoll separation and MACS in combination, a population of cells that was 95% PNA^+ ionocytes was obtained. By contrast, the

purity of the PNA^+ cell fraction obtained by FACS in the present study was only slightly lower, at ~92%. Examination of the PNA^+ cell fraction by confocal microscopy suggested that the impurities included a few cells that were not PNA^+ as well as some cellular debris. Whether methodological improvements could improve the purity of the resultant PNA^+ cell fraction remains to be determined. Such improvements might include separation of cellular debris from cells prior to sorting, possibly via centrifugation and/or density gradient centrifugation, addition of a second marker that would identify live cells, or the use of multiple passes of cell sorting. Although these strategies would likely improve the purity of the PNA^+ cell fraction obtained, they would also probably reduce the cell yield.

In summary, FACS using PNA as a label appears to be a viable method for isolating a high purity population of PNA^+ ionocytes from the trout gill epithelium. Other specific cell types clearly could also be isolated, as long as a fluorescent label that is specific for the cell type of interest is available. For example, the HR cell of the zebrafish gill could be isolated using concanavalin A as a specific marker (Horng et al., 2007). The use of multiple labels could provide an alternative route to isolate a cell population of interest for which a specific marker is not yet known. For example, dual labelling of dissociated trout gill cells with MitoTracker® and PNA would allow PNA^+ ionocytes to be separated from PNA^- ionocytes (Galvez et al., 2002). The main advantage of this approach is to allow a move away from carrying out measurements on tissue homogenates. Isolation of a specific cell type allows for the testing of hypotheses regarding the function of that cell type. As a proof-of-principle test of this approach, an experiment was carried out to determine the response of PNA^+ ionocytes to an acid-base challenge.

4.2 Responses of PNA$^+$ ionocytes to metabolic alkalosis

To investigate transcript responses of PNA$^+$ ionocytes to metabolic alkalosis, FACS was used to isolate populations of PNA$^+$ ionocytes from gill tissue of rainbow trout exposed to hypercapnic recovery or control conditions. This analysis revealed significantly higher relative mRNA abundance of *cac* in PNA$^+$ cells isolated from trout exposed to hypercapnic recovery than in PNA$^+$ cells from control trout, suggesting a role for transcriptional regulation of *cac* in PNA$^+$ cells in response to metabolic alkalosis. Similarly, Gilmour et al. (2011) reported significantly higher *cac* transcript abundance in the trout gill following metabolic alkalosis achieved by base infusion, but could not attribute this response to a particular ionocyte type because gill tissue was collected. In both cases, an increase in *cac* transcript abundance within the putative base-secreting cells of the gill epithelium was recognized as being an appropriate response to an alkalosis because it would be expected to facilitate base secretion (Gilmour and Perry, 2009; Goss et al., 2011; Boyle et al., 2015). Moreover, the occurrence of this response supports the notion of the PNA$^+$ ionocyte as a base-secreting cell. Whether the increase in transcript abundance reflects increased *cac* transcription within existing cells, an increase in PNA$^+$ cell numbers owing to cell proliferation stimulated by alkalosis, or a combination of these factors remains to be determined. Unfortunately, technical challenges associated with maintaining the flow of dissociated trout gill cells through the FACS instrument meant that in most cases, cell sorting occurred in multiple episodes, precluding accurate cell counts from being acquired. If these problems cannot be overcome in future trials, then an alternative approach will be needed to determine whether the number of PNA$^+$ ionocytes increases in response to systemic alkalosis. The time-differential double fluorescent staining technique (Katoh and Kaneko, 2003; Mitrovic and Perry, 2009) could be used for this purpose. Interestingly, Brannen and Gilmour (2018)

using immunohistochemistry did not detect a significant increase in PNA^+ ionocyte number in response to alkalosis achieved through recovery from hypercapnia. This observation suggests that transcriptional control of *cac* is more important than proliferation of CAc-containing PNA^+ ionocytes.

The increase in *cac* transcript abundance is also the most likely culprit to explain the increased abundance of CAc positive PNA^+ ionocytes observed by Brannen and Gilmour (2018). Although Brannen and Gilmour (2018) reported that only a low percentage of PNA^+ cells was CAc-positive on the basis of immunohistochemical detection of CAc, the *cac* transcript abundance of PNA^+ cells under control conditions was comparable to that of the 'negative' cell fraction in the present study, possibly suggesting that PNA^+ cells express CAc but at a low level that is not easily detected by immunohistochemistry. Brannen and Gilmour (2018) also reported decreases in the abundance of PNA^- ionocytes as well as CAc-positive PNA^- ionocytes during recovery from hypercapnia. A decrease in CAc transcript abundance in PNA^- ionocytes, which are acid-secreting cells (Galvez et al., 2002; Reid et al., 2003; Goss et al., 2011) would be an appropriate response to metabolic alkalosis (Gilmour and Perry, 2009). Although no effect of alkalosis was detected on *cac* transcript abundance in the 'negative' cell fraction of the present study, it is important to recognize that this fraction included both PNA^- ionocytes and other cell types, such as mucus cells, pavement cells and neuroepithelial cells, that are not expected to play a role in acid-base regulation (Evans et al., 2005).

As expected, the transcript abundance of *nka* in PNA^+ ionocytes was significantly greater than that of the 'negative' cell fraction. Not only did the 'negative' cell fraction consist largely of cells that are not ionocytes and hence not enriched in NKA, but NKA abundance and activity are higher in PNA^+ ionocytes than in PNA^- ionocytes (Galvez et al., 2002; Hawkings et al.,

2004). The relative mRNA abundance of *nka* also was significantly higher in PNA^+ ionocytes from trout exposed to metabolic alkalosis than in PNA^+ ionocytes from control trout, suggesting a transcriptional response of *nka* to metabolic alkalosis. This result was unexpected because acid-base compensation during an alkalosis is expected to rely on base excretion coupled to Cl^- uptake, with roles for CAc in providing HCO_3^- to be excreted via the catalyzed hydration of CO_2 and possibly a basolateral H^+-ATPase that would export protons generated by hydration of CO_2, but no obvious role for NKA (Tresguerres et al., 2006; Gilmour and Perry 2009). Indeed, NKA was selected essentially as a negative control for the cellular response to alkalosis of PNA^+ ionocytes. The strong transcriptional response of *nka* to alkalosis suggests that its role in base excretion requires re-evaluation, particularly in light of the evidence supporting the presence of NHE in PNA^+ ionocytes (Ivanis et al., 2008; Hiroi and McCormick, 2012).

Consistent with previous studies that have placed NHE2 and NHE3 in PNA^+ ionocytes using immunohistochemistry (Ivanis et al., 2008; Hiroi and McCormick, 2012), transcript abundances of *nhe2* and *nhe3* were significantly higher in PNA^+ ionocytes than in the 'negative' cell fraction. The presence of NHE2 and NHE3 in a cell type of the trout gill epithelium that has been implicated in base excretion remains unexpected, particularly given that these exchangers have been placed in acid-secreting ionocytes in other freshwater fish species such as zebrafish, tilapia and medaka (Hiroi et al., 2008; Inokuchi et al., 2009; Hsu et al., 2014; Guh et al., 2015). Neither *nhe2* nor *nhe3* exhibited a transcriptional response to alkalosis, consistent with their expected roles in Na^+ uptake and H^+ excretion (Wright and Wood, 2009; Kumai and Perry, 2011).

4.3 Perspectives

The findings of the present study demonstrate that FACS is an effective technique for isolation of specific ionocyte populations of the trout gill epithelium, and the proof-of-principle experiment further demonstrates the utility of this approach in studying the branchial responses to an acid-base challenge. In comparison to previous methods used to isolate ionocyte populations, such as the multi-step Percoll density gradient separation followed by MACS developed by Goss and colleagues (Galvez et al., 2002), or the laser capture microdissection approach utilized by Leguen et al. (2015), FACS is relatively straightforward. The importance of such techniques is evident given the increasing number of studies reporting multiple ionocyte types in diverse fish species and the associated need to assess each ionocyte type individually to characterize its transporter complement, function, and responses to acid-base and ionic challenges (Goss et al., 2001; Hiroi et al., 2008; Inokuchi et al., 2009; Hwang et al., 2011; Dymowska et al., 2012; Hsu et al., 2014; Guh et al., 2015). The findings of the present study also support and extend the results of Gilmour et al. (2011), where a transcriptional response of gill *cac* to metabolic alkalosis was reported but could not be attributed to a specific ionocyte type, and Brannen and Gilmour (2018), where changes in the abundance of CAc-positive PNA^+ ionocytes were reported but the underlying mechanisms were not evaluated. Collectively, these studies led to the question of whether transcriptional up-regulation of *cac* occurs specifically in PNA^+ ionocytes in response to an alkalosis. Utilizing FACS to isolate PNA^+ ionocytes from the gill epithelium of alkalotic trout, the present study confirmed that transcription of *cac* in PNA^+ ionocytes is increased following alkalosis. In conclusion, although further refinement of the experimental approaches developed in the present study is still needed, the study has

demonstrated the feasibility and utility of FACS as a method to study the function of ionocyte subtypes in the branchial epithelium of freshwater fish.

REFERENCES

Arora M. 2013. Cell Culture Media: A Review. *Mater Methods* 3: 1-29.

Bonner WA, Hulett HR, Sweet RG, Herzenberg LA. 1971. Fluorescence activated cell sorting. *Rev Sci Instrum* 43: 404-409.

Boone CD, Pinard M, McKenna R, Silverman D. 2014. Catalytic mechanism of α-class carbonic anhydrases: CO_2 hydration and proton transfer. In: *Carbonic Anhydrase: Mechanism, Regulation, Links to Disease, and Industrial Applications*, edited by Frost SC, McKenna R. Dordrecht, Netherlands: Springer Science+Business Media, 75: 31-52.

Brannen M, Gilmour KM. 2018. Carbonic anhydrase expression in the branchial ionocytes of rainbow trout. *J Exp Biol* 221: 1-9.

Castro R, Bromage E, Abós B, Pignatelli J, González Granja A, Luque A, Tafalla C. 2014. CCR7 is mainly expressed in teleost gills, where it defines an IgD^+ IgM^- B lymphocyte subset. *J Immunol* 192: 1257-1266.

Claiborne JB, Edwards SL, Morrison-Shetlar AI. 2002. Acid-base regulation in fishes: cellular and molecular mechanism. *J Exp Zool* 293: 302-319.

Clarke AP, Potts WTW. 1998. Isolated filament potentials and branchial ion fluxes in the European flounder. Evidence for proton pump mediated sodium uptake. *J Zool, Lond* 246: 433-442.

Darzynkiewicz Z, Roederer M, Tanke H. 2004. Cytometry, 4th Edition: New Developments. Elsevier, USA. 1-876.

.

Dymowska AK, Hwang P-P, Goss GG. 2012. Structure and function of ionocytes in the freshwater fish gill. *Respir Physiol Neurobiol* 184: 282-292.

Emmons C, Kurtz I. 1994. Functional characterization of three intercalated cell subtypes in the rabbit outer cortical collecting duct. *J Clin Invest* 93: 417-423.

Esbaugh AJ, Perry SF, Bayaa M, Georgalis T, Nickerson J, Tufts BL, Gilmour KM. 2005. Cytoplasmic carbonic anhydrase isozymes in rainbow trout Oncorhynchus mykiss: comparative physiology and molecular evolution. *J Exp Biol* 208: 1951-1961.

Etzler ME. 1986. Distribution and function of plant lectins. *The Lectins: Properties, Functions, and Applications in Biology and Medicine*. Academic Press, USA 371-425.

Evans DH, Piermarini PM, Choe KP. 2005. The multifunctional fish gill: dominant site of gas exchange, osmoregulation, acid-base regulation, and excretion of nitrogenous waste. *Physiol Rev*. 85: 97-177.

Evers DL, Fowler CB, Cunningham BR, Mason JT, O'Leary TJ. 2011. The effect of formaldehyde fixation on RNA. *J Mol Diagn* 13: 282-289.

Feng S, Zhan W, Sheng X, Yang K, Han J, Wei J, Li J, Qiao X. 2009. Response of mucosal and systemic sIgM-positive cells in turbot (*Scophthalmus maximus* L.) immunization with *Edwardsiellatarda*. *Vet Immunol Immunopathol* 129: 108-114.

Galvez F, Reid SD, Hawkings G, Goss GG. 2002. Isolation and characterization of mitochondria-rich cell types from the gill of freshwater rainbow trout. *Am J Physiol* 282: R658-R668.

Gao XB, Eladari D, Leviel F, Tew BY, Miró-Julià C, Cheema FH, Miller L, Nelson R, Păunescu TG, McKee M, Brown D, Al-Awqati Q. 2010. Deletion of hensin/DMBT1 blocks conversion of β- to α-intercalated cells and induces distal renal tubular acidosis. *Proc Natl Acad Sci* 107: 21872-21877.

Georgalis T, Perry SF, Gilmour KM. 2006. The role of branchial carbonic anhydrase in acid-base regulation in rainbow trout (*Oncorhynchus mykiss*). *J Exp Biol* 209: 518-530.

Gilmour KM, Collier CL, Dey CJ, Perry SF. 2011. Roles of cortisol and carbonic anhydrase in acid-base compensation in rainbow trout, *Oncorhynchus mykiss*. *J Comp Physiol B* 181: 501-515.

Gilmour KM, Perry SF. 2009. Carbonic anhydrase and acid-base regulation in fish. *J Exp Biol* 212: 1647-1661.

Girard JP, Payan P. 1980. Ion exchanges through respiratory and chloride cells in freshwater- and seawater-adapted teleosteans. *Am J Physiol*. 238: 260-268.

Goss GG, Adamia S, Galvez F. 2001. Peanut lectin binds to a subpopulation of mitochondria-rich cells in the rainbow trout gill epithelium. *Am J Physiol* 281: R1718-R1725.

Goss G, Gilmour K, Hawkings G, Brumbach JH, Huynh M, Galvez F. 2011. Mechanism of sodium uptake in PNA negative MR cells from rainbow trout, *Oncorhynchus mykiss* as revealed by silver and copper inhibition. *Comp Biochem Physiol Part A Mol Integr Physiol* 159: 234-241.

Goss GG, Wood CM. 1990. Na^+ and Cl^- uptake kinetics, diffusive effluxes and acidic equivalent fluxes across the gills of rainbow trout. I. Responses to environmental hyperoxia. *J Exp Biol* 152: 521-547.

Hawkings GS, Galvez F, Goss GG. 2004. Seawater acclimation causes independent alterations in Na^+/K^+- and H^+-ATPase activity in isolated mitochondria-rich cell subtypes of the rainbow trout gill. *J Exp Biol* 207: 905-912.

Hiroi J, Yasumasu S, McCormick SD, Hwang P, Kaneko T. 2008. Evidence for an apical Na-Cl cotransporter involved in ion uptake in a teleost fish. *J Exp Biol* 211: 2584-2599.

Hsu H, Lin L, Tseng Y, Horng J, Hwang P. 2014. A new model for fish ion regulation: identification of ionocytes in freshwater- and seawater-acclimated medaka (*Oryzias latipes*). *Cell Tissue Res* 357: 225-243.

Hwang P-P, Lee T-H, Lin L-Y. 2011. Ion regulation in fish gills: recent progress in the cellular and molecular mechanisms. *Am J Physiol* 301: R28-R47.

Horng J, Lin L, Huang C, Katoh F, Kaneko T, Hwang P. 2007. Knockdown of V-ATPase A (*atp6v1a*) impairs acid secretion and ion balance in zebrafish (*Danio rerio*). *Am J Physiol* 292: R2068-R2076.

Inokuchi M, Hiroi J, Watanabe S, Hwang P, Kaneko T. 2009. Morphological and functional classification of ion-absorbing mitochondria-rich cells in the gills of Mozambique tilapia. *J Exp Biol* 212: 1003-1010.

Ivanis G, Esbaugh AJ, Perry SF. 2008. Branchial expression and localization of SLC9A2 and SLC9A3 sodium/hydrogen exchangers and their possible role in acid–base regulation in freshwater rainbow trout (*Oncorhynchus mykiss*). *J Exp Biol* 211: 2467-2477.

Kumai Y, Perry SF. 2011. Ammonia excretion via Rhcg1 facilitates Na^+ uptake in larval zebrafish, *Danio rerio*, in acidic water. *Am J Physiol* 301: R1517-R1528.

Laerum OD, Farsund T. 1981. Clinical Application of Flow Cytometry: a Review. *Cytometry* 2(1): 1-13.

LeHir M, Kaissling B, Koeppen BM, Wade JB. 1982. Binding of peanut lectin to specific epithelial cell types in kidney. *Am J Physiol Cell Physiol* 242: C117-C120.

Leguen I, Le Cam A, Montfort J, Peron S, Fautrel A. 2015. Transcriptomic analysis of trout gill ionocytes in fresh water and sea water using laser capture microdissection combined with microarray analysis. *PLOS ONE* 10(10): 1-22.

Livak KJ, Schmittgen TD. 2001. Analysis of relative gene expression data using real-time quantitative PCR and the 2(-Delta Delta C(T)) Method. *Methods* 24(4): 402-408.

Maren TH. 1967. Carbonic anhydrase: chemistry, physiology and inhibition. *Physiological reviews* 47: 595-781.

Nawata CM, Hung CC, Tsui TK, Wilson JM, Wright PA, Wood CM. 2007. Ammonia excretion in rainbow trout (*Oncorhynchus mykiss*): evidence for Rh glycoprotein and H^+ -ATPase involvement. *Physiol Genomics* 31: 463-474.

Novogrodsky A, Lotan R, Ravid A, Sharon N. 1975 Peanut agglutinin, a new mitogen that binds to galactosyl sites exposed after neuraminidase treatment. *J Immunol* 115: 1243-1248.

Osman M, Ruch J. 1981. Behavior of odontoblasts and basal lamina of trypsin or EDTA-isolated mouse dental papillae in short-term culture. *J Dent Res* 60: 1015-1027.

Pan Q, Ye L, Deng Z, Li L, Liu H. 2014. Effects of red blood cells lysing solutions on the detection of peripheral basophils of healthy normals and SLE patients by flow cytometry. *J Immunoassay Immunochem* 35: 368-377.

Parks DR, Herzenberg LA. 1984. Fluorescence-activated cell sorting: Theory, experimental optimization, and applications in lymphoid cell biology. *Methods Enzymol* 108: 197-241.

Parks SK, Tresguerres M, Goss GG. 2009. Cellular mechanisms of Cl^- transport in trout gill mitochondrion-rich cells. *Am J Physiol* 296: R1161-R1169.

Parks SK, Tresguerres M, Galvez F, Goss GG. 2010. Intracellular pH regulation in isolated trout gill mitochondrion-rich (MR) cell subtypes: Evidence for Na^+/H^+ activity. *Comp Biochem Physiol Part A Mol Integr Physiol* 155: 139-145.

Peracchia C. 1977. Gap junctions. Structural changes after uncoupling procedures. *J Cell Biol* 72: 628-641.

Perry SF. 1997. The chloride cell: structure and function in the gills of freshwater fishes. *Annu Rev Physiol* 59: 325-347.

Perry SF, Gilmour KM. 2006. Acid-base balance and CO_2 excretion in fish: Unanswered questions and emerging models. *Respir Physiol Neurobiol* 154: 199-215.

Perry SF, Goss GG. 1994. The effects of experimentally altered gill chloride cell surface area on acid-base regulation in rainbow trout during metabolic alkalosis. *J Comp Physiol B* 164: 327-336.

Reid SD, Hawkings GS, Galvez F, Goss GG. 2003. Localization and characterization of phenamil-sensitive Na+ influx in isolated rainbow trout gill epithelial cells. *J Exp Biol* 206: 551-559.

Schwartz GJ, Barasch J, Al-Awqati Q. 1985. Plasticity of functional epithelial polarity. *Nature* 318: 368-371.

Shao J, Dabrowski MJ, White CC, Kavanagh TJ, Gallagher EP. 2010. Flow cytometric analysis of BDE 47 mediated injury to rainbow trout gill epithelial cells. *Aquat Toxicol* 97: 42-50.

Star RA, Burg MB, Knepper MA. 1985. Bicarbonate secretion and chloride absorption by rabbit cortical collecting ducts. *J Clin Invest* 76: 1123-1130.

Tresguerres M, Katoh F, Orr E, Parks SK, Goss GG. 2006. Chloride uptake and base secretion in freshwater fish: a transepithelial ion-transport metabolon? *Physiol Biochem Zool* 79(6): 981-996.

Tsui TKN, Hung CYC, Nawata CM, Wilson JM, Wright PA, Wood CM. 2009. Ammonia transport in cultured gill epithelium of freshwater rainbow trout: the importance of Rhesus glycoproteins and the presence of an apical Na^+/NH_4^+ exchange complex. *J Exp Biol* 212: 878-892.

Vogel KG. 1978. Effects of hyaluronidase, trypsin, and EDTA on surface composition and toporaphy during detachment of cells in culture. *Exp Cell Res* 113(2): 345-357.

Wolff A, Perch-Nielsen IR, Larsen UD, Friis P, Goranovic G, Poulsen CR, Kutter JP, Telleman P. 2003. Integrating advanced functionality in a microfabricated high-throughput fluorescent-activated cell sorter. *Lab Chip* 3: 22-27.

Zadunaisky JA. 1996. Chloride cells and osmoregulation. *Kidney Int* 49: 1563-1567.